



Calhoun: The NPS Institutional Archive
DSpace Repository

NPS Scholarship

Theses

1975-03

Modeling an input-output geokinetic system utilizing a finite element approach.

Foos, Robert Charles

Monterey, California. Naval Postgraduate School

<https://hdl.handle.net/10945/20944>

This publication is a work of the U.S. Government as defined in Title 17, United States Code, Section 101. Copyright protection is not available for this work in the United States.

Downloaded from NPS Archive: Calhoun



Calhoun is the Naval Postgraduate School's public access digital repository for research materials and institutional publications created by the NPS community. Calhoun is named for Professor of Mathematics Guy K. Calhoun, NPS's first appointed -- and published -- scholarly author.

Dudley Knox Library / Naval Postgraduate School
411 Dyer Road / 1 University Circle
Monterey, California USA 93943

<http://www.nps.edu/library>

MODELING AN INPUT-OUTPUT GEOKINETIC SYSTEM
UTILIZING A FINITE ELEMENT APPROACH

Robert Charles Foos

Library
Naval Postgraduate School
Monterey, California

NAVAL POSTGRADUATE SCHOOL

Monterey, California



THESIS

MODELING AN INPUT-OUTPUT GEOKINETIC SYSTEM
UTILIZING A FINITE ELEMENT APPROACH

by

Robert Charles Foos

March 1975

Thesis Advisors:

Donald R. Barr
Rex H. Shudde

Approved for public release; distribution unlimited.

T168187

REPORT DOCUMENTATION PAGE		READ INSTRUCTIONS BEFORE COMPLETING FORM
1. REPORT NUMBER	2. GOVT ACCESSION NO.	3. RECIPIENT'S CATALOG NUMBER
4. TITLE (and Subtitle) Modeling an Input-Output Geokinetic System Utilizing a Finite Element Approach		5. TYPE OF REPORT & PERIOD COVERED Master's Thesis; March 1975
7. AUTHOR(s) Robert Charles Foos		6. PERFORMING ORG. REPORT NUMBER
9. PERFORMING ORGANIZATION NAME AND ADDRESS Naval Postgraduate School Monterey, California 93940		8. CONTRACT OR GRANT NUMBER(s)
11. CONTROLLING OFFICE NAME AND ADDRESS Naval Postgraduate School Monterey, California 93940		10. PROGRAM ELEMENT, PROJECT, TASK AREA & WORK UNIT NUMBERS
14. MONITORING AGENCY NAME & ADDRESS (if different from Controlling Office) Naval Postgraduate School Monterey, California 93940		12. REPORT DATE March 1975
		13. NUMBER OF PAGES
		15. SECURITY CLASS. (of this report) Unclassified
		15a. DECLASSIFICATION/DOWNGRADING SCHEDULE
16. DISTRIBUTION STATEMENT (of this Report) Approved for public release; distribution unlimited.		
17. DISTRIBUTION STATEMENT (of the abstract entered in Block 20, if different from Report)		
18. SUPPLEMENTARY NOTES		
19. KEY WORDS (Continue on reverse side if necessary and identify by block number) Finite Element Earth Surface Tilt Tidal Ocean Loading Geokinetics		
20. ABSTRACT (Continue on reverse side if necessary and identify by block number) The modeling research presented in this paper of an input-output geokinetic system can be applied to problems not only in earthquake research but also to problems in siloed missile systems. The finite element technique provides an effective methodology for exploring the detailed surface movements of the earth in response to ocean tidal loading. The finite element computer program utilized in this paper was especially designed		

for analyzing deformations and strains resulting from a system of loads applied to a structure. Relationships are explored between surface loads and fault zone tilt response as a function of fault zone shear strength, and distance of the fault from the load.

Modeling an Input-Output Geokinetic System
Utilizing a Finite Element Approach

by

Robert Charles Foos
Captain, United States Army
B.S., United States Military Academy, 1969

Submitted in partial fulfillment of the
requirements for the degree of

MASTER OF SCIENCE IN OPERATIONS RESEARCH

ABSTRACT

The modeling research presented in this paper of an input-output geokinetic system can be applied to problems not only in earthquake research but also to problems in siloed missile systems. The finite element technique provides an effective methodology for exploring the detailed surface movements of the earth in response to ocean tidal loading. The finite element computer program utilized in this paper was especially designed for analyzing deformations and strains resulting from a system of loads applied to a structure. Relationships are explored between surface loads and fault zone tilt response as a function of fault zone shear strength, and distance of the fault from the load.

TABLE OF CONTENTS

I.	INTRODUCTION-----	8
II.	FINITE ELEMENT MODEL CONTRASTED WITH BOUSSINESQ MODEL-----	11
III.	DEVELOPMENT OF RELATIONSHIPS BETWEEN FAULT ZONE TILT, FAULT LOCATION, FAULT SHEAR STRENGTH AND SURFACE LOADS-----	15
IV.	MODELS OF FOUR PROFILES OF THE CALIFORNIA COASTLINE-----	31
V.	AREAS FOR FURTHER STUDY-----	38
VI.	CONCLUSIONS-----	39
APPENDIX A	- DOCUMENTATION OF THE FINITE ELEMENT COMPUTER PROGRAM-----	40
APPENDIX B	- LISTING OF FINITE ELEMENT TECHNIQUE COMPUTER PROGRAM-----	57
BIBLIOGRAPHY	-----	77
INITIAL DISTRIBUTION LIST	-----	79

LIST OF TABLES

TABLE I	-----	19
TABLE II	-----	20
TABLE III	-----	24

LIST OF FIGURES

1.	FINITE ELEMENT STRUCTURE AND LOAD-----	12
2.	LOCATION MAP OF U.S. GEOLOGICAL SURVEY SEISMOGRAPH STATIONS AND MAJOR FAULTS IN CENTRAL CALIFORNIA-----	18
3.	FAULT ZONE TILT, SOFT BOTTOM MODEL-----	20
4.	FAULT ZONE TILT, HARD BOTTOM MODEL-----	21
5.	FAULT ZONE TILT, STEWART MODEL-----	22
6.	FAULT ZONE SHEAR MODULUS, SOFT BOTTOM MODEL-----	26
7.	FAULT ZONE SHEAR MODULUS, HARD BOTTOM MODEL-----	27
8.	FAULT ZONE SHEAR MODULUS, STEWART MODEL-----	28
9.	FIGURE OF DISPLACEMENT FIELD IN THE HARD BOTTOM MODEL-----	30
10.	FOUR CALIFORNIA PROFILES-----	53
11.	PROFILE A-----	34
12.	PROFILE B-----	35
13.	PROFILE C-----	36
14.	PROFILE D-----	37
15.	FIVE MESH TYPES-----	42
16.	SAMPLE OF COMPLETED GRID DESIGN-----	45

I. INTRODUCTION

This study explores modeling a specific input-output system in the field of geokinetics. A finite element technique is utilized as the system simulator. The Earth's surface movements are the output to several geophysical phenomena. One of the most significant geophysical inputs is ocean tital loading. Finite element modeling provides an effective technique for exploring the detailed surface movements of the earth in response to ocean loading.

The first chapter of this paper discusses the bounds of the finite element model. The finite element model is contrasted with an analytical half space Boussinesq technique in order to provide the level of detail which should be included in the finite element model. Tilts resulting from two and three dimensional surface loads on the Boussinesq half space models bracket the tilt produced by the two dimensional finite element model. In the second chapter relationships are explored between surface loads and fault zone tilt response as a function of fault zone shear strength, and distance of the fault from the load. The results indicate a logarithmic relationship between the magnitude of fault zone tilt and distance of the fault from the load. The final chapter describes four profiles of the California coastline in an attempt to relate real data collected by the United States Geological Survey to model results.

It is assumed that the reader is already familiar with solving families of differential equations by finite difference techniques and their applications to geophysical sciences. Only token consideration is given in this paper to the theory of finite difference techniques and their application to finite element modeling. The reader unfamiliar with finite element methodology is encouraged to read the appendix of this paper containing the documentation of the finite element computer program. This documentation should give the reader a better perception of the finite element modeling technique. There are also several excellent references published on the subject of finite element techniques [1, 9, 15].

There are many applications of the finite element technique besides solving geophysically related systems. The pure research which is presented in this paper can be applied to problems not only in earthquake research but, for example, also in air defense missile systems [2]. Accurately predicted ground motion near siloed missiles can be programmed into the missile's prelaunch parameters of the inertial guidance system. This information results in fewer course corrections required for the missile and therefore a higher probability of hitting its target.

The finite element computer program utilized in this paper was especially designed for analyzing deformations and strains resulting from a system of loads applied to a structure. This two dimensional finite element computer program was developed at the National Center for Earthquake Research of the United

States Geological Survey by Dr. James H. Dieterich [3], Dr. M. Darroll Wood and refined by the author. The author is greatly indebted to Dr. M. Darroll Wood for his cooperation, guidance and geophysics expertise which made this paper possible. The terminology and notation used in this paper was adopted from Dr. Wood's doctoral thesis [12]. The author also expresses his appreciation to Professor Donald Barr and Professor Rex Shudde for their helpful criticism and ideas during the stages of development of this paper. The William R. Church Computer Center was a tremendous asset in the cooperation and service which it provided in processing the finite element computer programs.

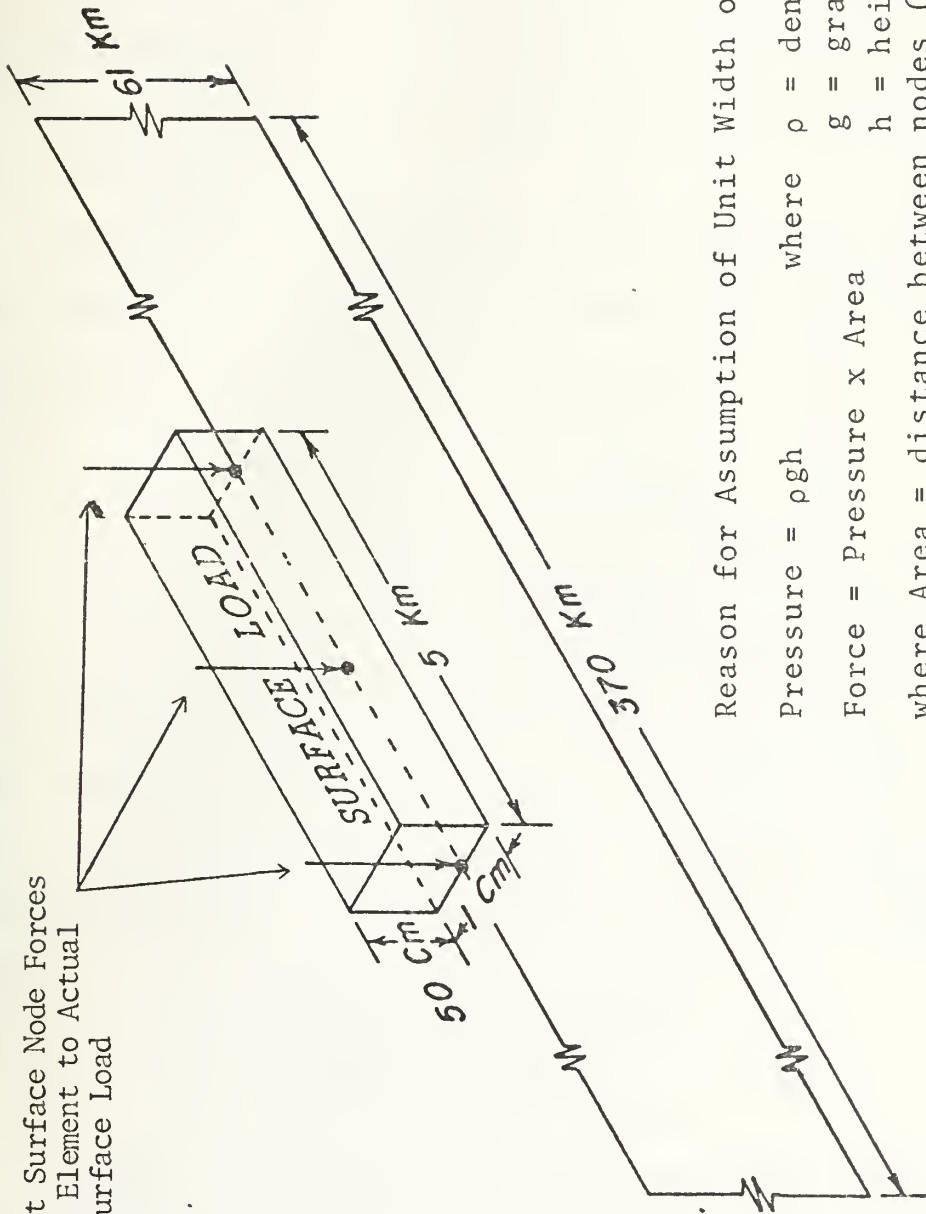
II. FINITE ELEMENT MODEL CONTRASTED WITH BOUSSINESQ MODEL

In 1878, Boussinesq calculated the vertical deviation of an elastic plane surface of a homogeneous medium under the loading effect caused by water. He showed that the vertical displacement of the Earth's crust was proportional at each point to the gravitational potential of the load and was a function of the elastic constants of the medium [8]. The Boussinesq technique has long been used as a simple approximation of load tilt. Load tilt is principally the gradient of the displacement field of the Earth's surface and two other secondary effects. The principal effect and the one which the finite element model simulates is that of the variable flexure of the Earth's crust under the loading effect caused by the oceans. The other effects are the attraction of the masses of water causing a vertical displacement of the Earth's surface, and the variation of the potential due to secondary deformation of the Earth's crust, an effect which is opposite in direction to the first and second effects [8].

The finite element structure is a two dimensional model in which the load is assumed to have unit width (Fig. 1). For this reason, it is difficult to directly compare the finite element model with Boussinesq half space models. The tilts calculated from the Boussinesq technique bounded the tilt produced from the finite element model in each of six

Finite Element Structure and Load

Equivalent Surface Node Forces
of Finite Element to Actual
Uniform Surface Load



Reason for Assumption of Unit Width of Surface Load

Pressure = $\rho g h$ where ρ = density of water

Force = Pressure x Area g = gravity

where Area = distance between nodes (length of

load) multiplied by a unit depth.

FIGURE 1

cases processed with different loads and elastic parameters. The finite element model overestimated the tilt calculated from the equivalent Boussinesq model with a two dimensional load, and consistently underestimated the tilt calculated from the equivalent Boussinesq model with a three dimensional load. The following description is of one model processed by the finite element model and the calculations associated with the Boussinesq method.

The Boussinesq method describes load tilt δ_x^l as the deviation of the vertical $\delta_x^a(r)$ due to a load of radial extent r multiplied by the Boussinesq factor m . Thus:

$$\delta_x^l = \delta_x^a(r) \cdot m \text{ where } m = \frac{\lambda + 2\mu}{4\pi(\lambda + \mu)\mu} \cdot \frac{g^2}{G}$$

where μ = shear modulus
 λ = modulus of rigidity (Lamé
 g = gravity Constants)
 G = gravitational constant.

The deviation of the vertical $\delta_x^a(r)$ due to a load of extent r and height h is the ratio of the horizontal gravity g_x to the vertical gravity attraction [12]. For the three dimensional

$$\text{Boussinesq model } \delta_x^a(r) = \frac{G \rho h}{g} \frac{d}{dx} \int \frac{dr}{r} = \frac{G \rho h}{g} \ln(r)$$

where ρ = density of load (water)
 G = gravitational constant
 h = height of the load
 g = gravity (vertical)
 r = radial extent of load.

For the two dimensional Boussinesq model $\delta_x^a(r)$ is computed using a line integral. Thus, $\delta_x^a(r) = \frac{G \rho h}{g \cdot r}$ where ρ , G , h , g , r are the same as above [12].

The finite element model was programmed to use the same inputs as the Boussinesq models of a homogeneous medium

containing elastic parameters $\lambda = \mu = 6.2 \times 10^{11}$ dynes/cm² (Lamé constants).

To simulate the Boussinesq boundary conditions, the bottom edge of the finite element structural model was specified as rigid. The load was a symmetrical surface load of water one centimeter in height and five kilometers in length.

The tilt calculated at the load center of the finite element model was 3.85×10^{-10} radians. The three dimensional Boussinesq method produced a load tilt of 2.47×10^{-9} radians, and the two dimensional Boussinesq methods produced a load tilt of 3.77×10^{-16} radians.

Because of the consistency with which the finite element model was bracketed by the Boussinesq methods, it is presumed that the finite element program will be a useful tool for detailed analysis of deformations resulting from a variety of loads applied to inhomogeneous structures. In order to have continuity throughout this paper, the bottom edges of remaining finite element models were structurally designed rigid.

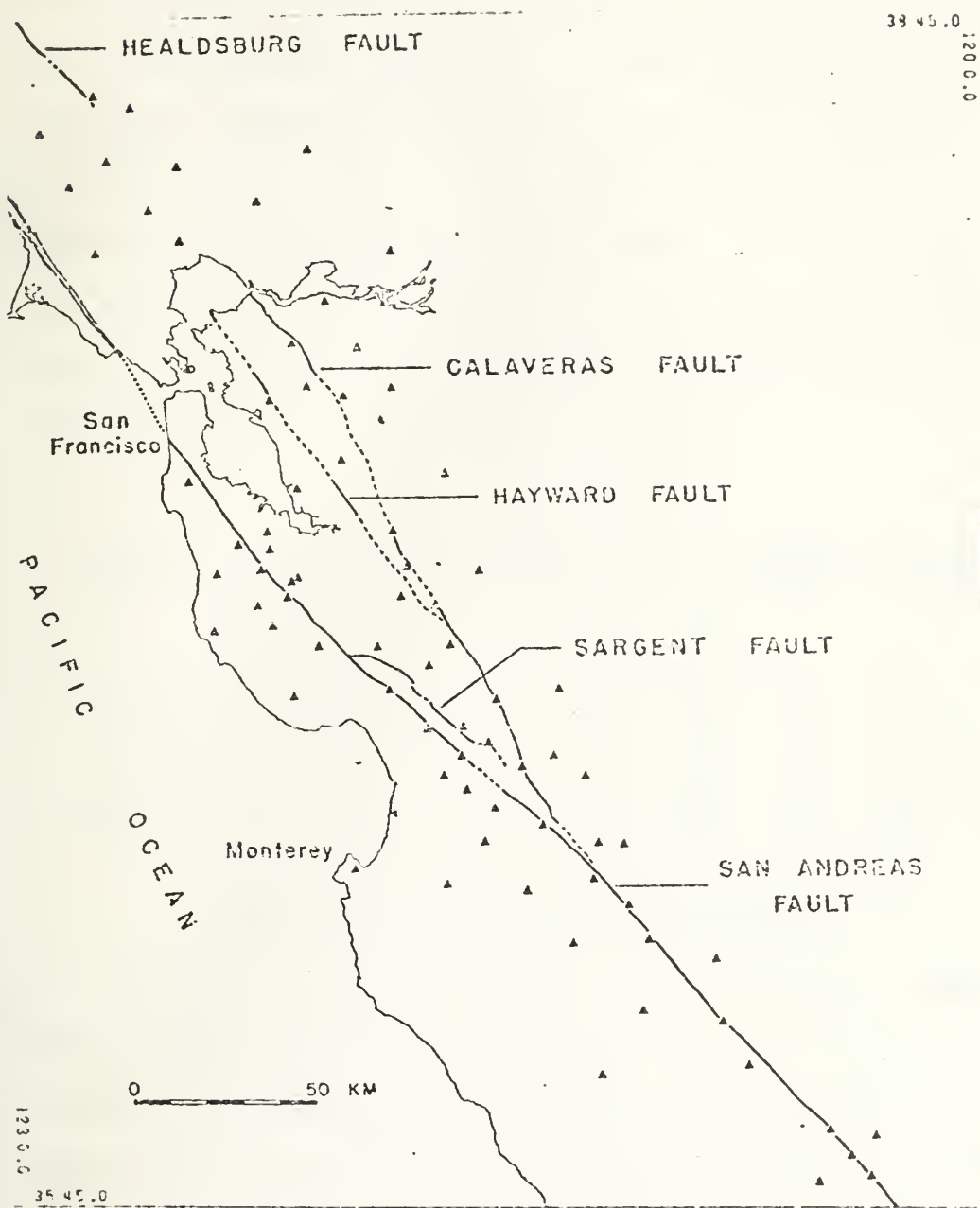
III. DEVELOPMENT OF RELATIONSHIPS BETWEEN FAULT ZONE TILT, FAULT LOCATION, FAULT SHEAR STRENGTH AND SURFACE LOADS

The response of earth structures to surface loads was explored utilizing the deterministic finite element model. The finite element model simulates the behavior of a discontinuous structure under asymmetric loading. The model structure was matched to the real Earth structure by laterally and vertically varying the known inhomogeneities of the earth. The response of the region near a vertical discontinuity, namely a fault, was of particular interest. The smallest homogeneous elements of the model were assumed to behave elastically for small increments of stress. However, the shear that is distributed in and near the fault zone elements or cells in the finite element grid may have varied considerably due to the contrast in Lamé constants for adjoining elements. The large difference in shear produces steps in the displacement field and therefore poses a problem of smoothness.

Tilt measurements in borehole and observatory sites have been made along the California coastline. Tilt measurements at tidal sensitivities (10^{-8} μ radians) show the Earth's surface response to oceanic loading is greater than responses from any other continuous source [13]. Conceivably, ocean loading constitutes a forcing function that can be used to derive the bulk elastic properties of the Earth. However, it has been shown that ocean tidal spectra are non-stationary

in all but lunar frequencies. The lunar semi-diurnal wave (M_2) is theoretically 85% of the energy of the total theoretical tidal spectrum [8]. In actuality this is not true. However, the M_2 line is sufficiently energetic and sufficiently removed from the contaminated tidal spectrum to be used as a stationary forcing function for earth response studies. For these reasons, the model surface load corresponded to the amplitude of the M_2 frequency. A value of fifty-three centimeters for the M_2 amplitude was chosen to represent the ocean loading in the central and northern California region [14]. In order to remain within the required aspect ratio in each cell of the finite element grid of 10:1 and to account for approximately 95% of the ocean loading effect as calculated by Boussinesq, the length of the load was chosen to be 165 kilometers [8]. With this loading, the investigation was limited to exploring relationships between fault zone tilt, fault shear strength, and the distance from the load to the fault. A factorial arrangement was developed by processing three slightly different velocity structure models having twelve fault locations and four fault shear moduli. The width and depth of the fault zone were set at five and sixteen kilometers respectively. These dimensions conform with Mayer-Rosa's [7] conclusion that the fault zone must be a low velocity zone at least several kilometers wide, extending into the lower crust. The fault zone was shifted consecutively in five kilometer increments from the edge of the load (coastline) to 60 kilometers inland.

This range of distances spans the extent of separation between the San Andreas Fault and the Pacific Ocean throughout most of central and northern California (Fig. 2). At each fault zone location, the shear strength of the fault was varied by adjusting the shear modulus in the fault zone. Starting with values of fault zone shear modulus set equal to adjacent elements, and then in consecutive models reducing the shear modulus in the fault zone one order of magnitude decrements, a maximum difference of four orders of magnitude less of shear strength in the fault zone was achieved.



Location map of U.S. Geological Survey seismograph stations and major faults in central California.

FIGURE 2

The Lamé constants computed for each cell were derived from studies of the seismic velocity models of Stewart [11] and the works he referenced. Three slightly different velocity structures were developed to observe differences in fault zone tilt response. The Poisson ratio was adjusted from 0.4 at the surface of the model to 0.25 at depths below ten kilometers. The density was derived using a Nafe-Drake curve. The three velocity models are represented by their associated elastic parameters in Table I.

TABLE I

DEPTH	HARD BOTTOM MODEL		SOFT BOTTOM MODEL		STEWART MODEL			
					GABILAN		DIABLO	
	λ	μ	λ	μ	λ	μ	λ	μ
1.0	0.28	0.12	0.28	0.12	0.28	0.12	1.1	4.5
6.0	2.3	1.5	2.3	1.5	1.6	1.0	2.3	1.5
16.0	3.3	3.3	3.3	3.3	3.3	3.3	3.3	3.3
26.0	4.3	4.3	4.3	4.3	4.3	4.3	4.3	4.3
41.0	6.5	6.5	6.5	6.5	6.5	6.5	6.5	6.5
61.0	6.5	6.5	1.1	0.45	6.5	6.5	6.5	6.5

λ and μ are in units of 10^{11} dynes/cm².
 Depths are in units of kilometers.

Tilt was calculated as the maximum positive slope of displacement throughout each fault zone. The phase of tilt in which the displacement gradient is toward the load is taken as positive. By examining the results of the finite element model for these three velocity structures, a relationship between fault zone tilt and the distance from the load to the fault was hypothesized. The calculated tilt in the fault zone was plotted logarithmically against linear distance between the fault zone and the edge of the load (Fig. 3, 4, 5). For distances between 10 and 45 kilometers,

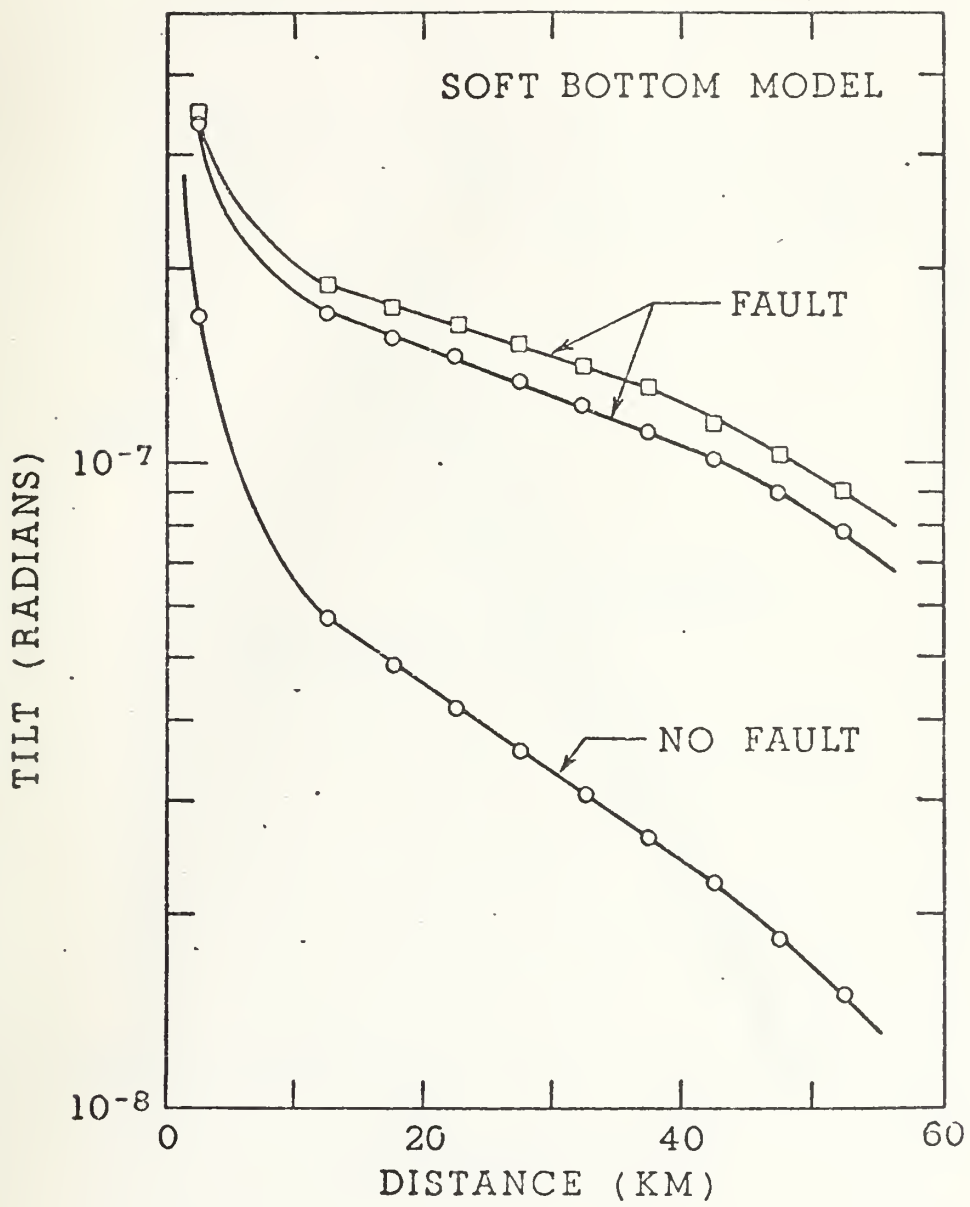


FIGURE 3

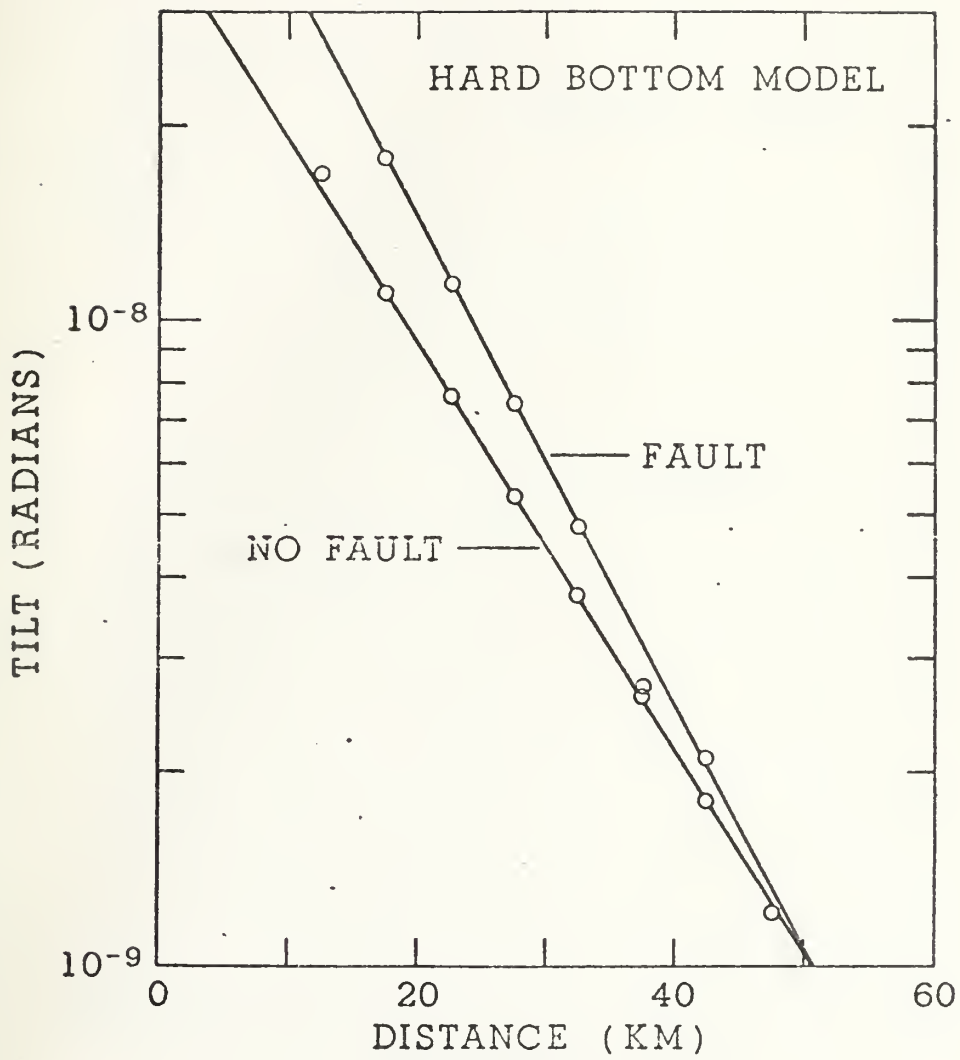


FIGURE 4

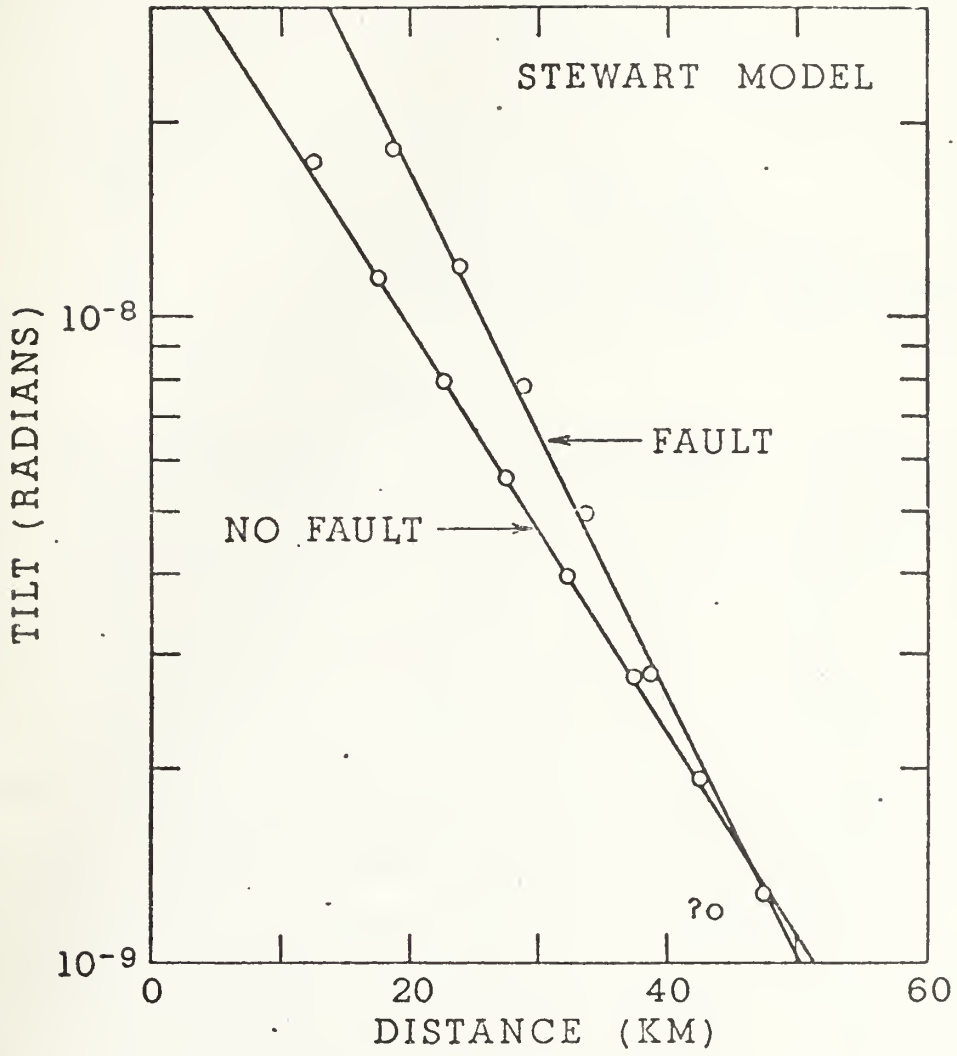


FIGURE 5

the tilt measurements lie nearly on a straight line for all three models and fault moduli. Straight lines on semi-logarithmic graph paper characterize the relationship as exponential. Equations describing the relationship between fault zone tilt and fault zone location are easily estimated from the graphs. The basic model is shown below, followed by Table II showing the value of each of the parameters for each velocity structure and fault shear strength.

$$T = T_0 e^{-s \cdot d}$$

where T = fault zone tilt
 T_0 = tilt intercept
s = slope of straight line
d = distance between fault zone and edge of the load (coastline)

TABLE II

	SOFT BOTTOM MODEL		HARD BOTTOM MODEL		STEWART MODEL	
	NO FAULT	FAULT	NO FAULT	FAULT	NO FAULT	FAULT
T_0	8.5×10^{-8}	2.15×10^{-7}	3.9×10^{-8}	8.0×10^{-8}	4.0×10^{-8}	1.1×10^{-7}
S	0.032	0.018	0.073	0.087	0.072	0.094
RANGE	5 < d < 50 km		10 < d < 50 km		10 < d < 45 km	

Tilt is strongly dependent on the shear modulus of the fault zone. When the shear modulus is decreased in the fault zone one order of magnitude from surrounding material, there is a distinct difference in the resulting tilt as compared with no fault structures. However, decreasing the shear modulus in the fault zone consecutively two, three and four orders of magnitude resulted in a small change of the fault zone tilt. This apparent convergence can best be seen from the table of calculated tilt in the fault zone for the three models (Table III). Plots of the shear modulus (μ) versus

TABLE III

FAULT ZONE	SOFT BOTTOM MODEL		HARD BOTTOM MODEL		STEWART MODEL			
	NO FAULT $\mu=10^9$	$\mu=10^8$	NO FAULT $\mu=10^9$	$\mu=10^8$	NO FAULT $\mu=10^9$	$\mu=10^8$	NO FAULT $\mu=10^7$	$\mu=10^6$
0-5	25.2	40.7	20.8	40.1	42.6	42.8	23.1	45.5
5-10	7.24	19.6	2.99	8.90	9.29	9.33	3.23	10.1
10-15	5.72	17.0	1.69	3.20	3.27	3.28	1.73	3.77
15-20	4.84	15.6	1.11	1.77	1.88	1.89	1.14	1.82
20-25	4.17	14.5	0.76	1.14	1.24	1.26	0.79	1.18
25-30	3.56	13.5	0.53	0.75	0.84	0.85	0.56	0.78
30-35	3.08	12.4	0.37	0.48	0.54	0.55	0.40	0.50
35-40	2.62	11.2	0.26	0.27	0.32	0.33	0.28	0.28
40-45	2.21	10.1	0.18	0.11	0.15	0.16	0.19	0.12
45-50	1.83	8.93	0.12	.004	0.02	0.03	0.13	*
50-55	1.51	7.82	0.08	*	*	*	0.08	*
55-60	1.20	*	0.05	*	*	*	0.05	*

Table contains tilt calculated in each fault zone location of three velocity structure models.

Tilt units (10^{-8} radians).

Fault zone is the distance from the edge of the load to fault zone (kilometers).

* Phase of tilt vector inverted.

fault zone tilt for each of the fault zone locations and velocity structures are shown in figures 6, 7, 8.

The dotted line segments of the graphs are the interesting feature. This part of the graph depicts the relationship between a no fault structure and a structure containing a fault zone of shear modulus decreased by one order of magnitude from surrounding material. There appears to be no similarities in this portion of the graphs for different fault zone locations. The dotted line portion of the graphs are flatter at fault zone locations further away from the load. The inference is that the more distant the loads, the less sensitive the response to a local discontinuity. Also, greater depths are required to adequately model distant loads. If the dotted lines in the graph are approximated as straight lines, then an equation relating the shear modulus to fault zone tilt is given by

$$T = A \cdot U^{-n}, \text{ where } \begin{array}{l} T = \text{fault zone tilt} \\ A = \text{tilt intercept} \\ U = \text{shear modulus of fault zone} \\ n = \text{slope of the straight line.} \end{array}$$

However, further study into particular fault zone locations is required before this equation can be verified.

There are several shortcomings in the modeling which has been presented. First, the soft bottom model is not a realistic representation of the Earth's velocity structure. However, this model does show a sensitivity with which fault zone tilt varies with slight changes in the overall velocity structure. The soft bottom model also unmistakably has the characteristic exponential relationship between fault zone

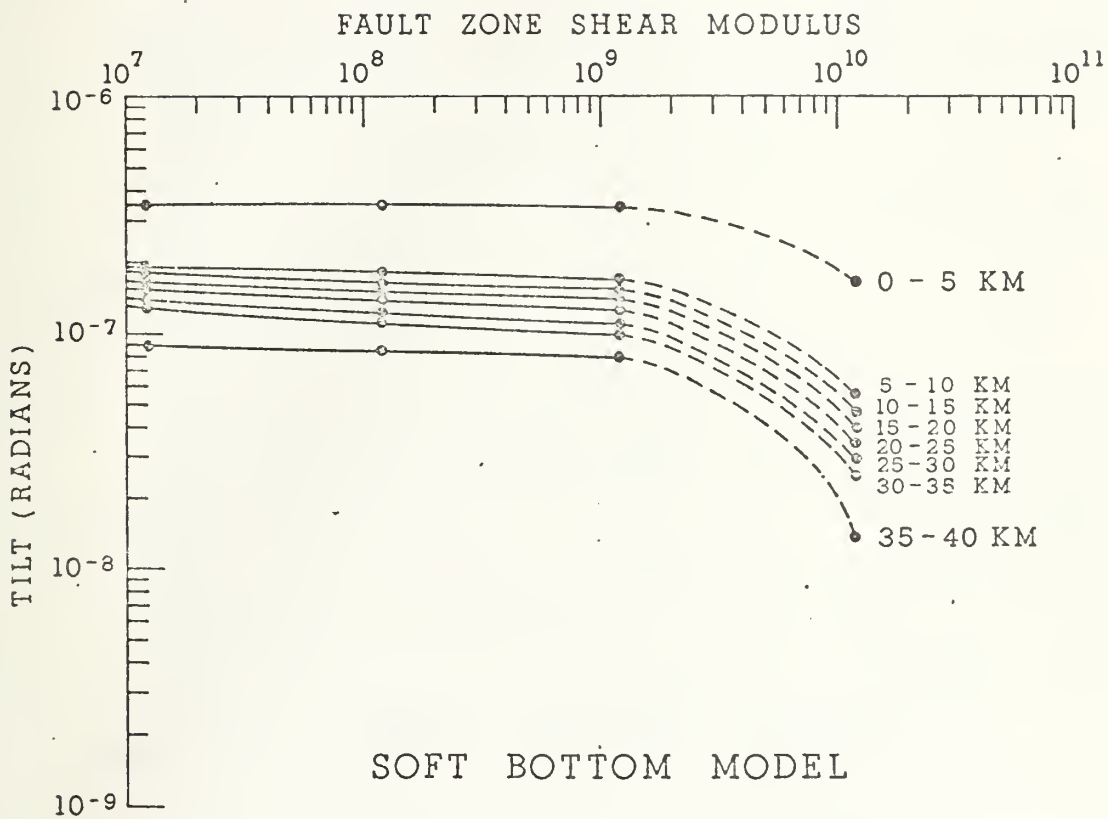


FIGURE 6

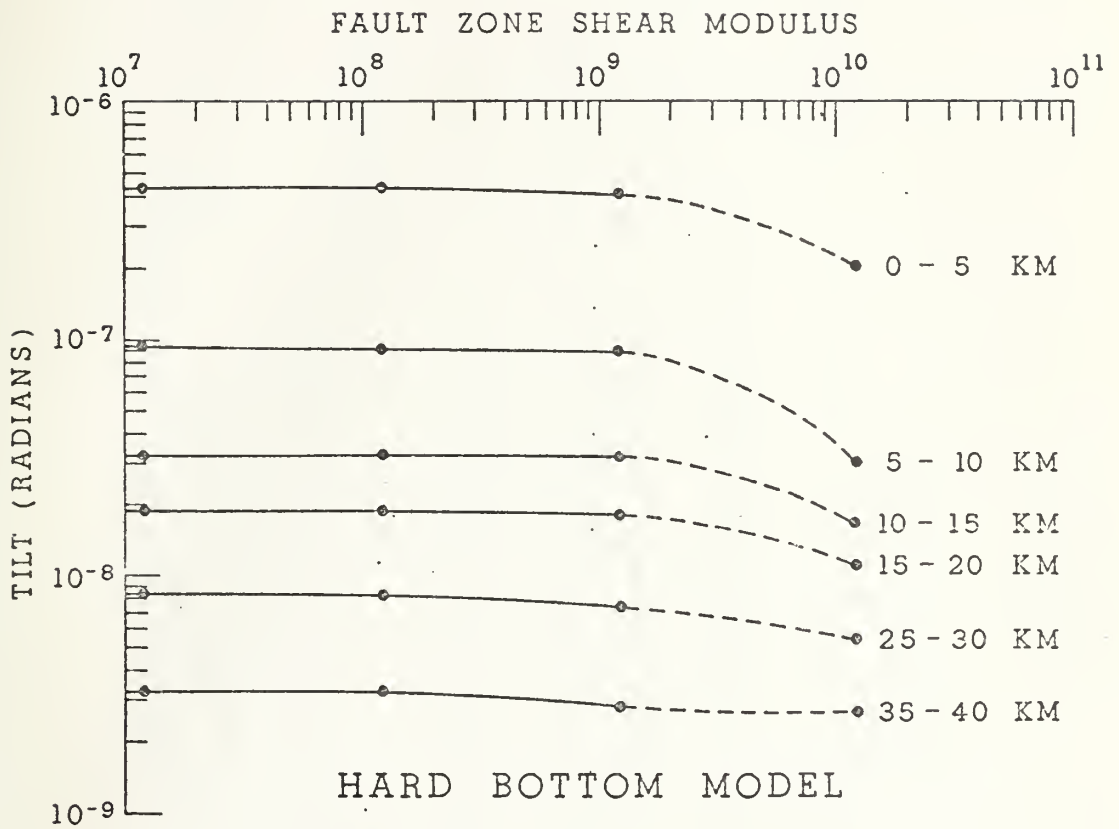


FIGURE 7

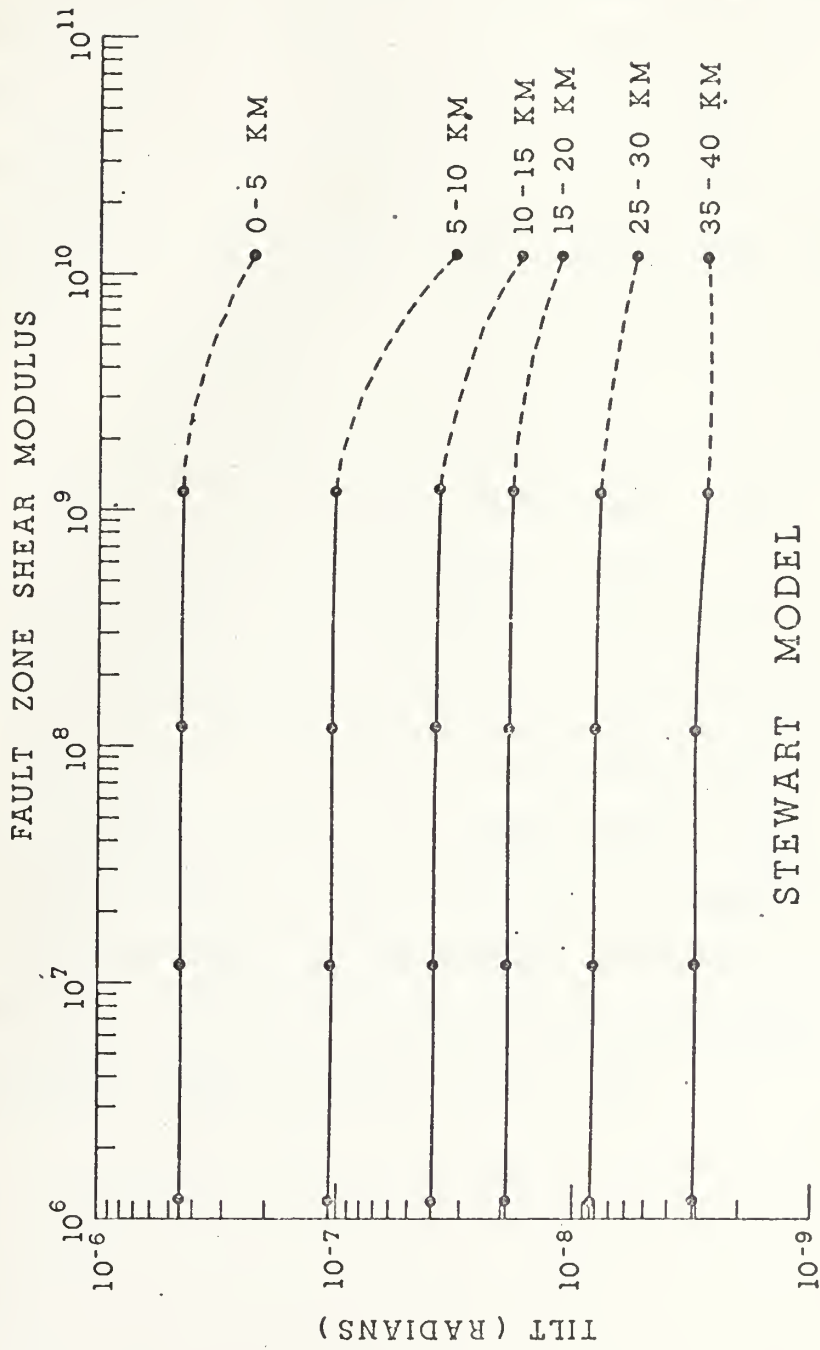


FIGURE 8

tilt and fault zone location in the range of 10 to 45 kilometers. Both the hard bottom model and the Stewart model are better models of the real Earth's velocity structure [11]. However, because of grid design constraints, the detail of the velocity structure which could be represented was limited, especially in the 0 to 15 kilometer depth range. A plot of the displacement field throughout the structure revealed a final shortcoming of the grid design. The depth used in the present model is too shallow to explore fault zone locations farther than 50 kilometers from the edge of the load. It is apparent from figure 9 that the problem of grid design is directly related to the boundary conditions of the rigid bottom edge. The rigid bottom has the tendency to make the next to bottom layer of the structure oscillate about zero centimeters displacement at distances over 50 kilometers from the load. Also, the ratio of effective distance of the load from a response point to the depth used in the model should not exceed unity. This deduction is demonstrated in figure 9 where the depth of the model structure is 61 kilometers and invalid results occurred beyond the region of 50 to 60 kilometers from the edge of the load.

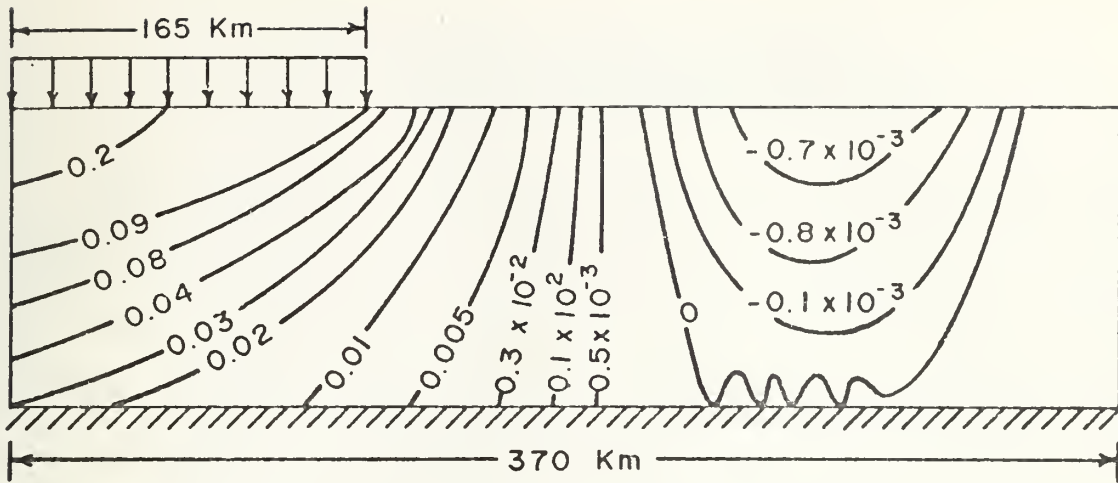


Figure of Displacement Field in the Hard Bottom Model

FIGURE 9

IV. MODELS OF FOUR PROFILES OF THE CALIFORNIA COASTLINE

Four profiles of the California coastline were modeled using the finite element technique in an attempt to compare the results with data collected by the United States Geological Survey. However, the results of these investigations point out pitfalls in the modeling phase. The four profiles are pictured in Figure 10. For reasons given below, the only useful profile is profile A. Figure 11 shows the displacement of the surface nodes plotted against distance. Figure 11 also depicts the location of the loading and the location of the fault zone. The upper dotted line results when a fault zone shear modulus is one order of magnitude less than the shear modulus of adjacent surface elements. The lower curve is based on the assumption that no fault zone exists and the elements in the fault zone are therefore identical with those adjacent to the zone at the same depth. The fault zone tilt associated with the no fault structure was 4.18×10^{-7} radians whereas the fault zone curve has a calculated tilt of 2.09×10^{-5} radians. This tilt was expected from the graphs developed in the previous chapter and is comparable to actual tilt data in the San Francisco Bay area. Figures 12, 13, 14 display the same attributes for profiles B, C, and D as that of Figure 11 of profile A. In profiles B, C, and D the ocean loading was not sufficient in magnitude to accurately model ground movement in these profiles. This resulted in the instabilities

discussed in the previous chapter. At least 165 kilometers or more of ocean loading is required to provide an adequate forcing function for the modeling of all profiles. Zones of 2.5 kilometers in width are probably too small to be realized by the existing grid design. Therefore, fault zones of 2.5 kilometers in width showed little or no change in the displacement field between no-fault and fault structures. Also, as stated in the previous chapter, the grid design is too shallow to place fault zones farther than 50 kilometers from the edge of the load and receive valid information.

FOUR CALIFORNIA PROFILES

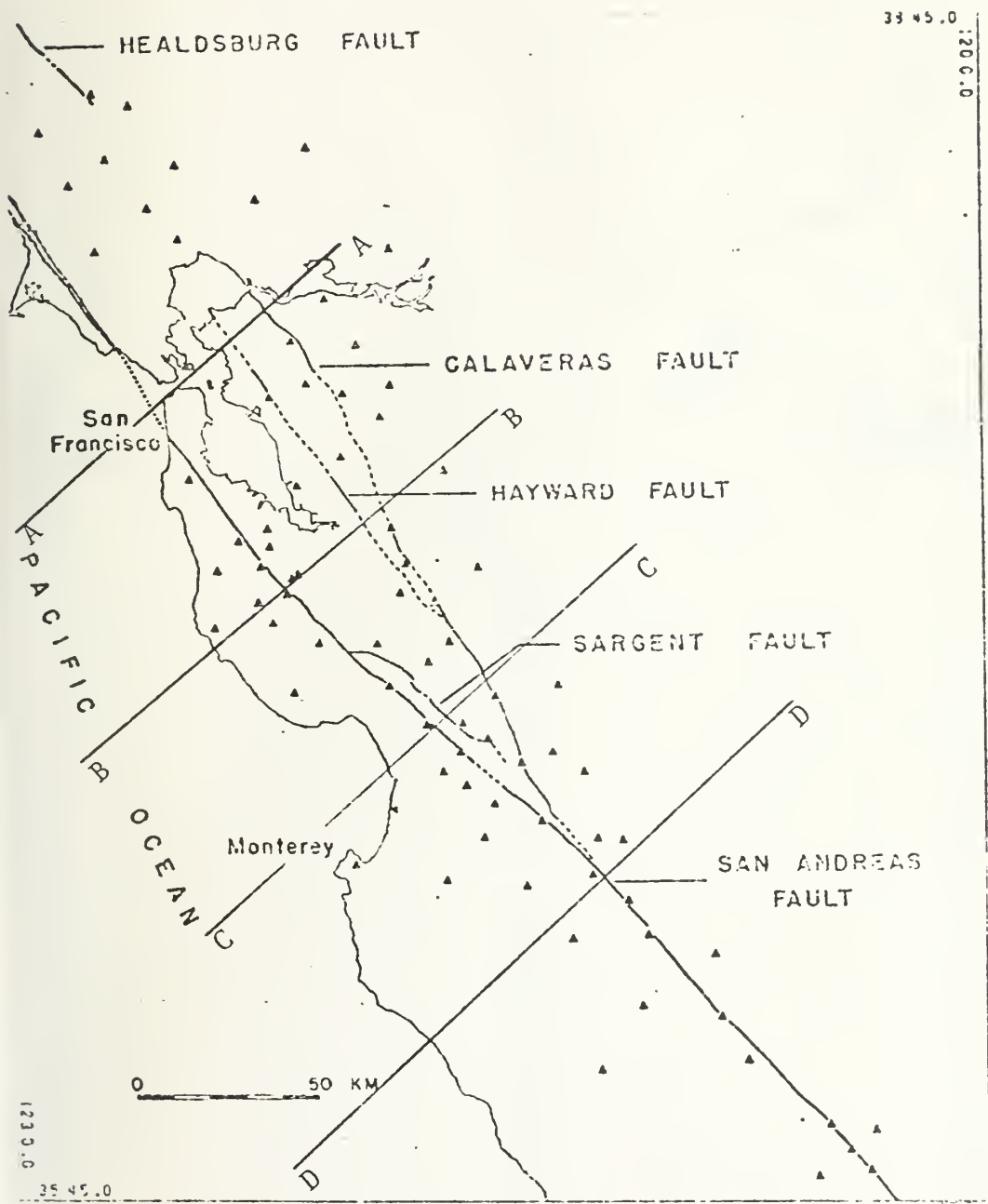


FIGURE 10

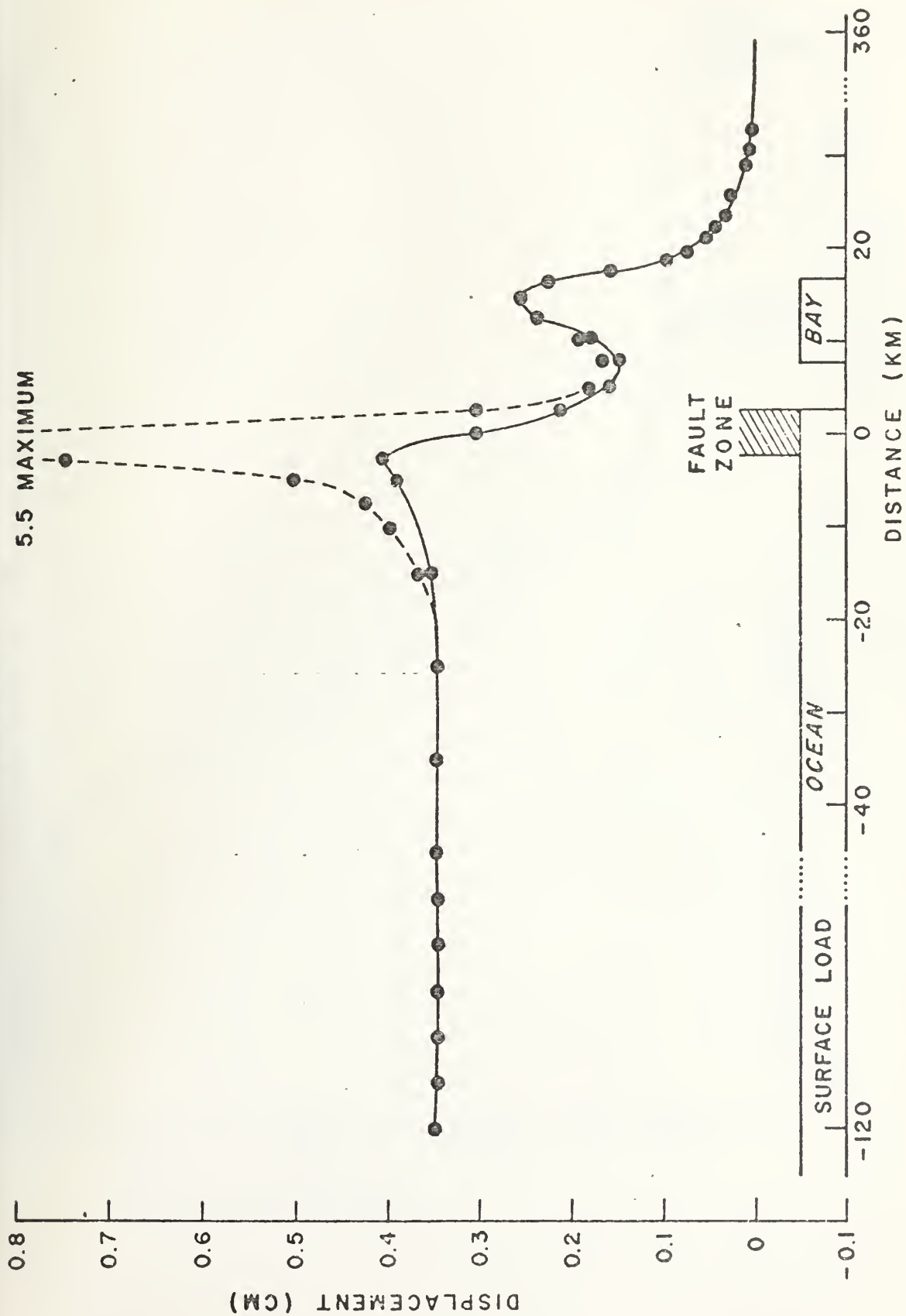


FIGURE 11

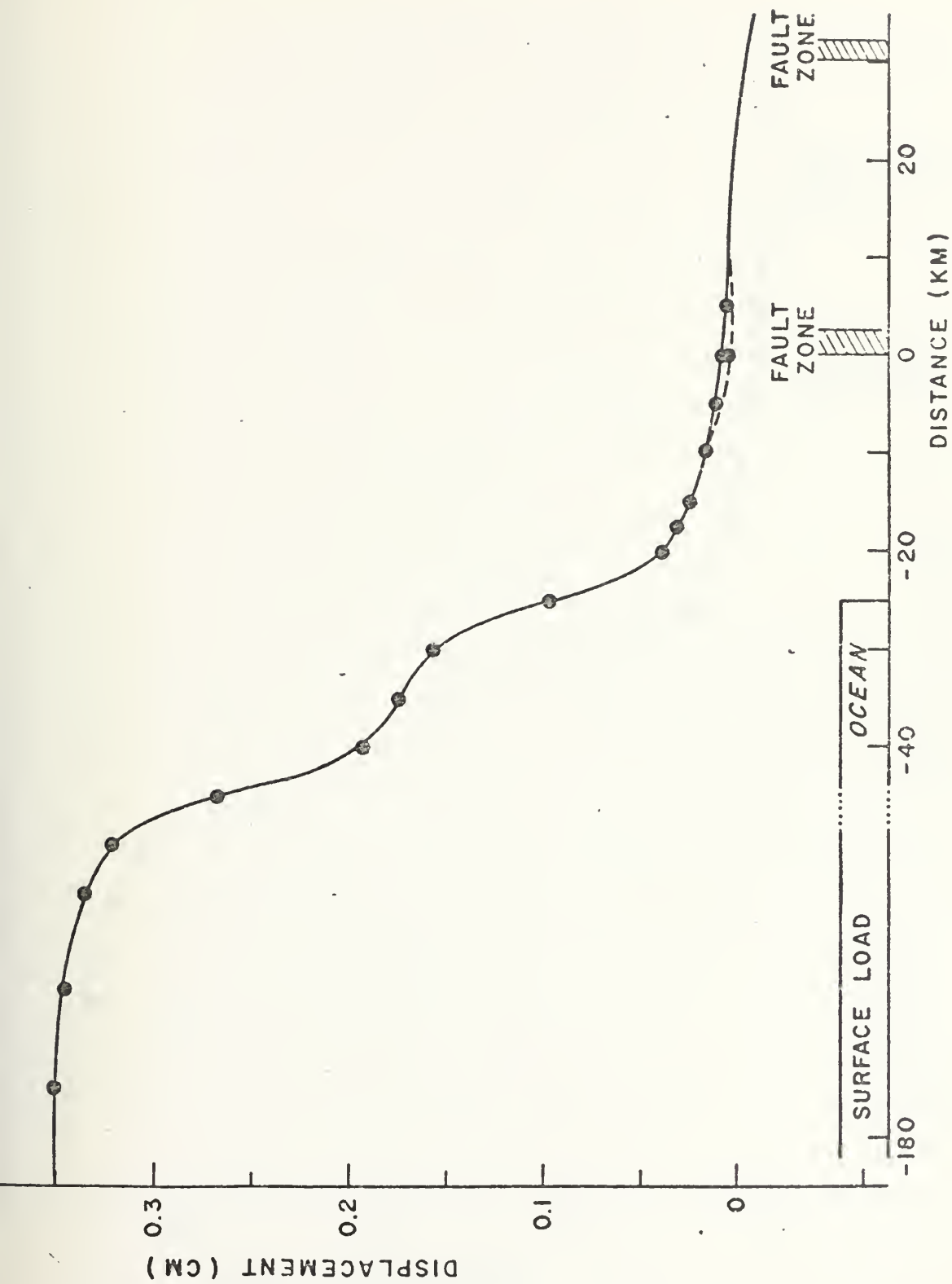


FIGURE 12

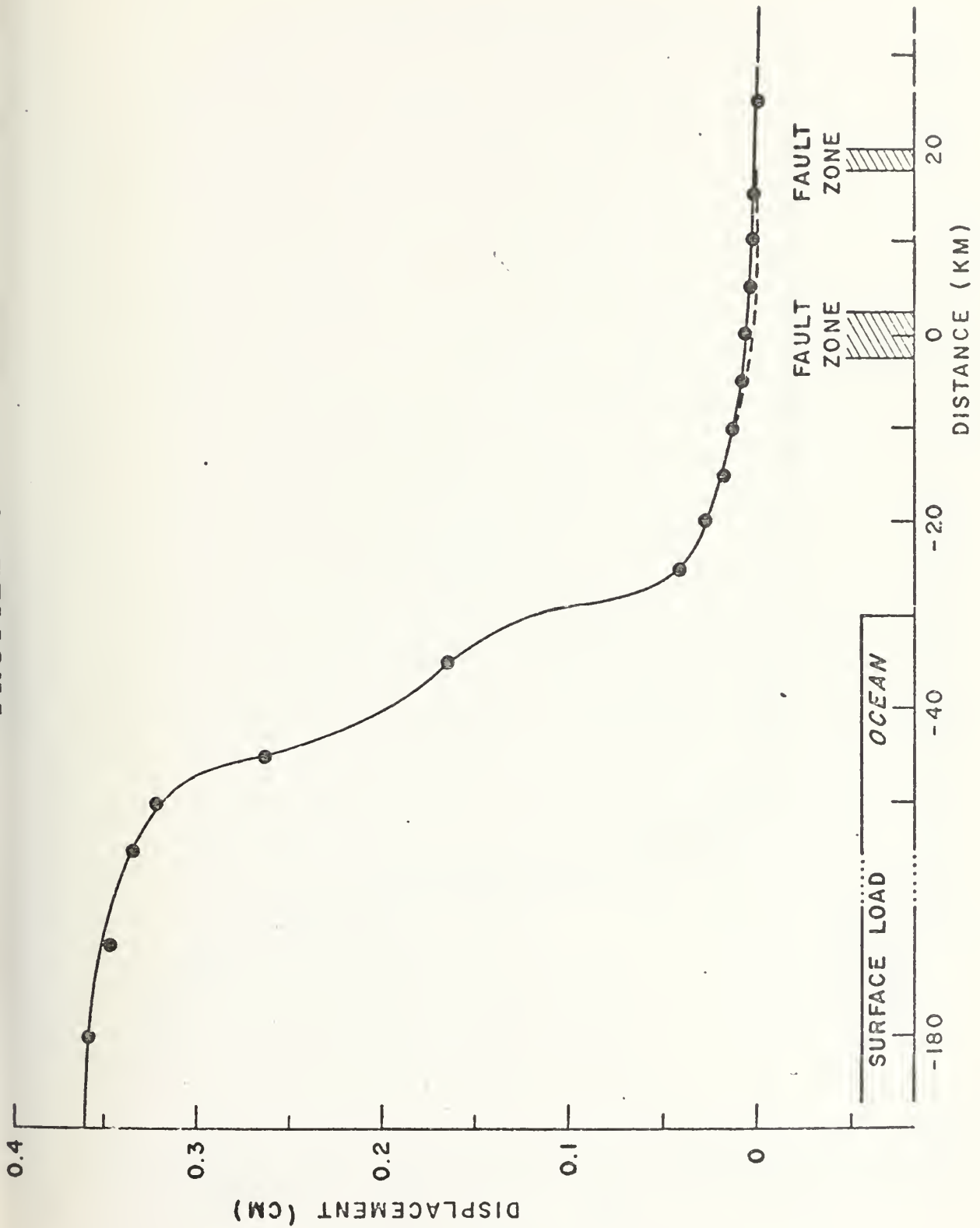


FIGURE 13

PROFILE D

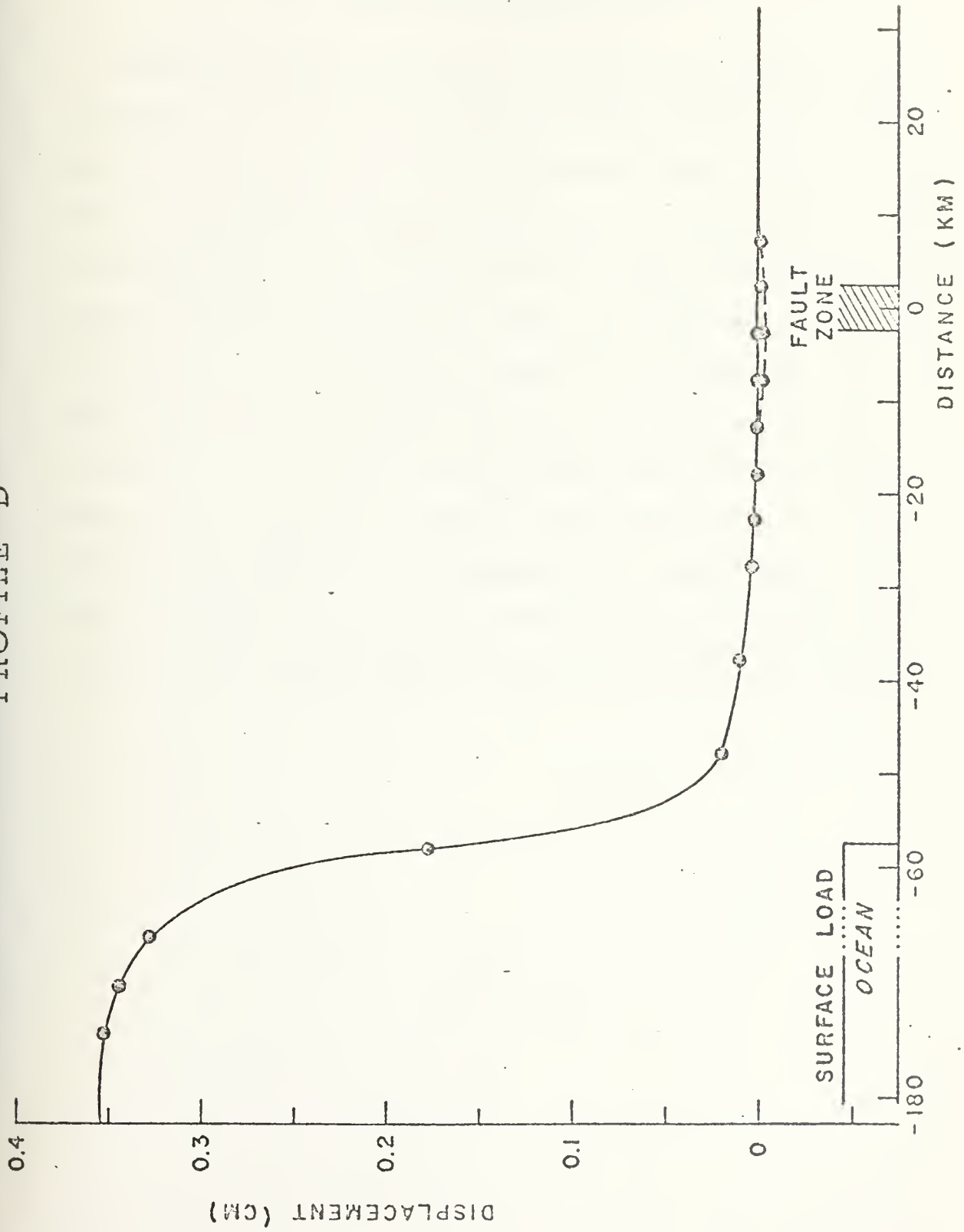


FIGURE 14

V. AREAS FOR FURTHER STUDY

Further study is definitely needed to develop the four California profiles into useable models. Modular construction of the grid is strongly encouraged when alterations are made to add further depth to the grid. Further work is needed to develop an effective and efficient three dimensional finite element computer program and model. This should provide a valuable tool for analyzing more detailed deformations resulting from a variety of loads applied to an inhomogeneous structure. This type of three dimensional finite element model could possibly be used in providing inputs to siloed missiles described in the introduction. Rainfall and barometric fluctuations could be used as the forcing functions to the finite element model instead of ocean tidal loading.

VI. CONCLUSIONS

The finite element model has demonstrated its usefulness in analyzing deformations resulting from a system of loads applied to an earth structure. If the structure is assumed to be of a homogeneous medium, then the finite element model produces results similar to that of Boussinesq models. In analyses of deformations in which the structure consists of an inhomogeneous medium the numerical method of finite elements has shown to be a most valuable asset. A logarithmic relationship between the magnitude of fault zone tilt and the distance of the fault zone from the edge of the load was shown to exist by manipulating the finite element model. Fault zone tilt was also shown to converge in magnitude for a given fault zone location when the fault zone shear modulus was decreased more than one order of magnitude from that of adjoining cells in the finite element grid.

APPENDIX A

DOCUMENTATION OF THE FINITE ELEMENT COMPUTER PROGRAM

The basic idea underlying the finite element concept is to substitute a simpler problem for the actual complex problem. If the simpler problem can be solved and if the resulting solution represents a feasible solution with acceptable accuracy, then the finite element technique has obviously served a useful purpose. The finite element method treats a continuum as an assembly of simple structural components or elements which are connected at a finite number of points, called nodes.

The process of fitting a variety of geophysical measurements to the array of possible earth structures and their responses requires a finite element technique. The finite element computer program used in this paper was developed to meet the need for a simple mesh or grid construction allowing for analysis of deformations of axisymmetric and plane strain elastic structures. The program is based on the theory of finite elements as presented by O. C. Ziekiewicz and Y. K. Cheung [15]. Typical finite element programs are so tedious and time consuming in the design of the mesh and indexing of the nodes and cells that they tend to inhibit a thorough investigation of the variety of models that satisfy the geophysical measurements. The finite element program in this paper solves the problems of inversion, non-uniqueness,

and convergence in an efficient and effective manner without becoming overly complex. The program has facilities for processing in one run, several models which the investigator requires for validating his hypotheses.

The computer program is written in Fortran. This facilitates using the program on different systems. The program is composed of a main program and two subroutines, named ASAPS and QPLOT.

The main program constructs the grid, indexes and positions nodes and cells, assigns associated elastic parameters, sets up boundary conditions, and places the vertical surface force in position. The construction of the grid is accomplished by the standardization of five modular mesh types. The mesh types are described as coarse, intermediate, fine, left and right link connectors. The five mesh types are shown in figure 15.

The grid is the hub of the modeling phase. It is constructed by assembling the five mesh types or any combination of mesh types into the desired structure. The dimensions of the grid may vary depending on the number of mesh types used. The grid may be designed so that nodal points are closer spaced by using the fine mesh type in areas where deformations are expected to vary most rapidly. To provide the appropriate transition from a coarse mesh to either an intermediate or fine mesh requires the appropriate right or left link connectors to be inserted. Figure 16 illustrates a completed grid design. The type of grid design which has been discussed

SAMPLE GRID MESH

Coarse

Intermediate

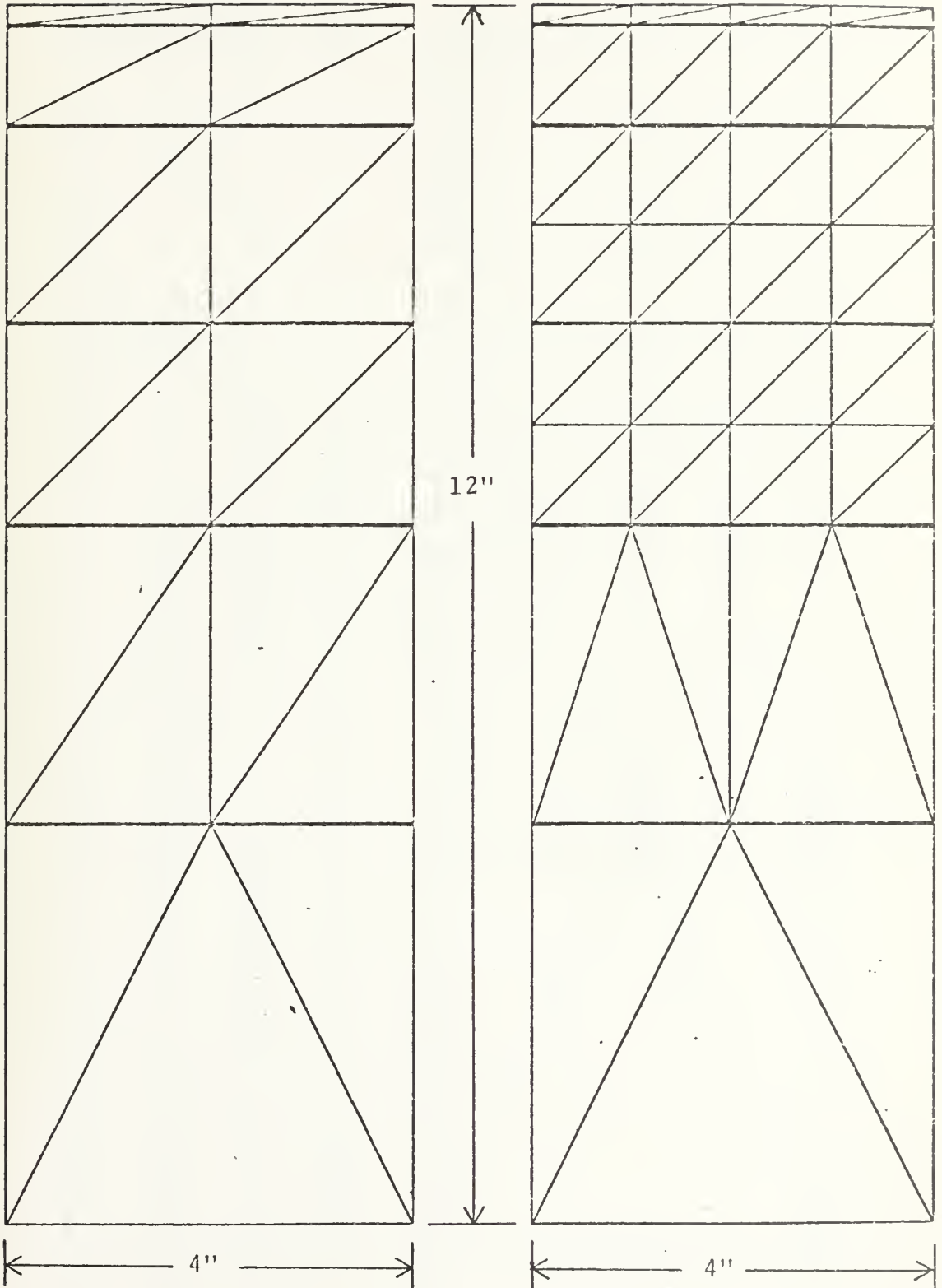
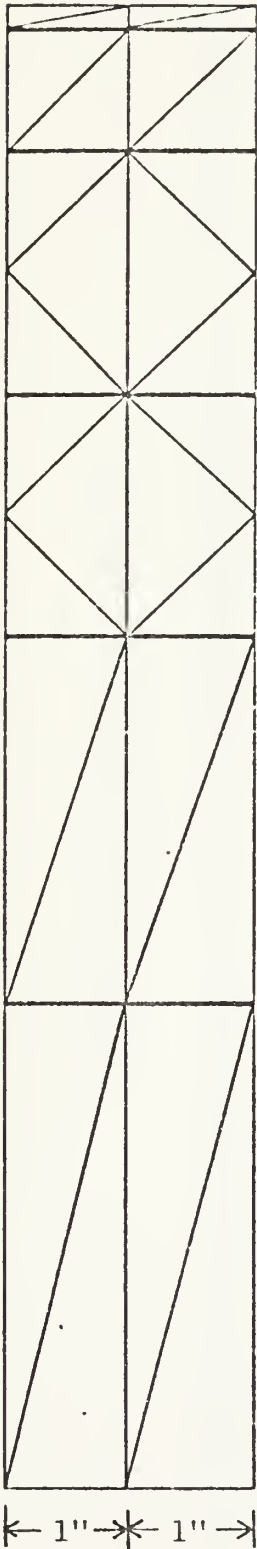


FIGURE 15A

SAMPLE GRID MESH

Right Link
Left Link



Fine

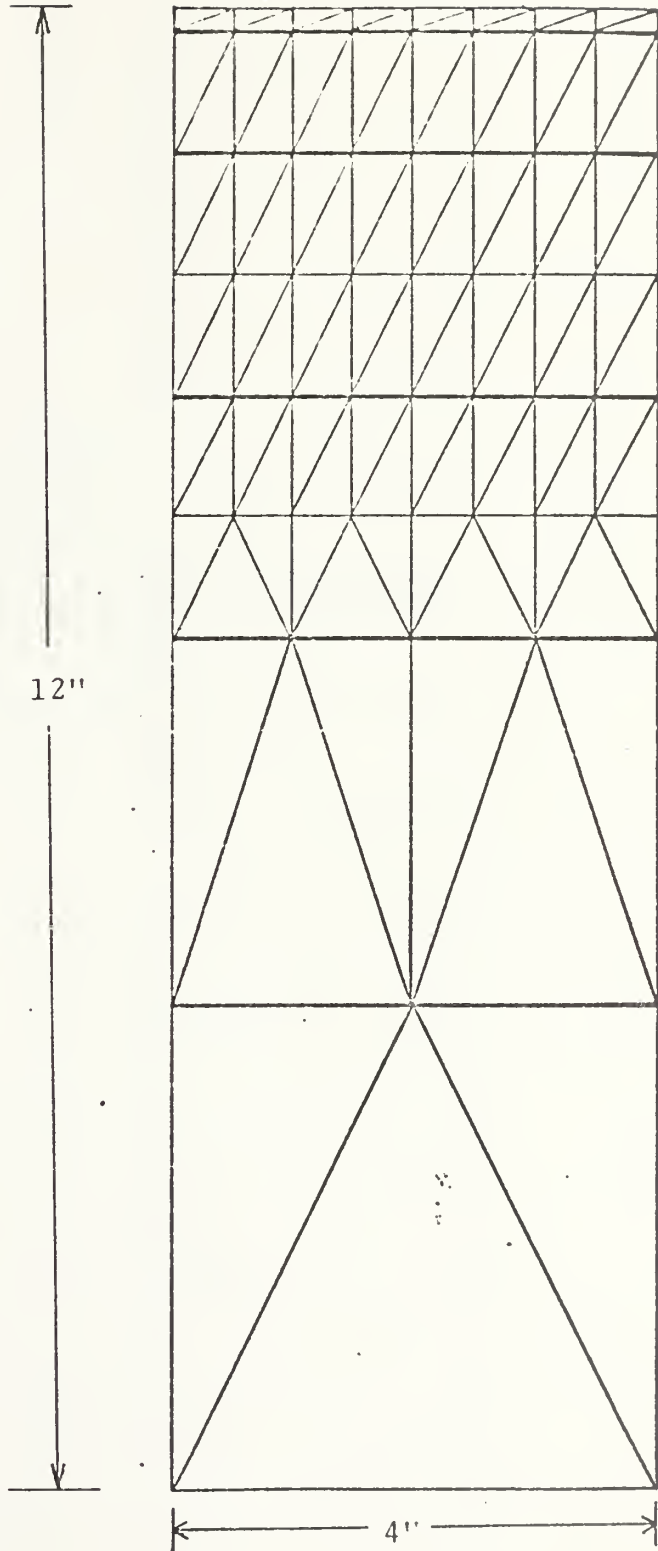


FIGURE 15B

above is only valid for plane strain modeling problems. Axisymmetric problems require a different type of grid which has ring-shaped elements with triangular cross sections. Thus for axisymmetric problems a manual grid construction is required and the automatic grid generator in the main program would be aborted. In any grid design the aspect ratio between the lengths of the two legs of the triangular element should not exceed 10:1.

An overlay procedure for elastic boundary conditions was devised so that structures composed of several materials are as easy to model as structures composed of a single material. Each elastic boundary condition is on a separate data card with the coordinates (in inches) which bound that particular set of elastic parameters. The overlay procedure is achieved by giving later specified boundary conditions precedence over former specified boundary conditions. This allows structures to be described by a basic structure which can be easily modified.

The ASAPS subroutine calculates the deformations of axisymmetric and plane-strain elastic structures, using the finite element technique [3]. This program employs the simple triangular element which is constrained to deform homogeneously (for axisymmetric problems the elements are ring-shaped with a triangular cross section). From the mechanical properties and dimensions of each element a stiffness matrix is formed for the entire assembly which relates nodal forces to nodal displacements. The x components and y components of nodal

displacements are the principal unknowns in the analysis and are determined from linear simultaneous equations of the form

$$F_t = \sum_{j=1}^{2N} K_{ij} D_j \quad i = 1, 2, \dots, 2N$$

where N = number of nodes

F_i = components of force at the nodes; F_i and F_{N+i} are the horizontal and vertical components of force, respectively, at the i^{th} node

K_{ij} = stiffness matrix

D_j = nodal displacement components.

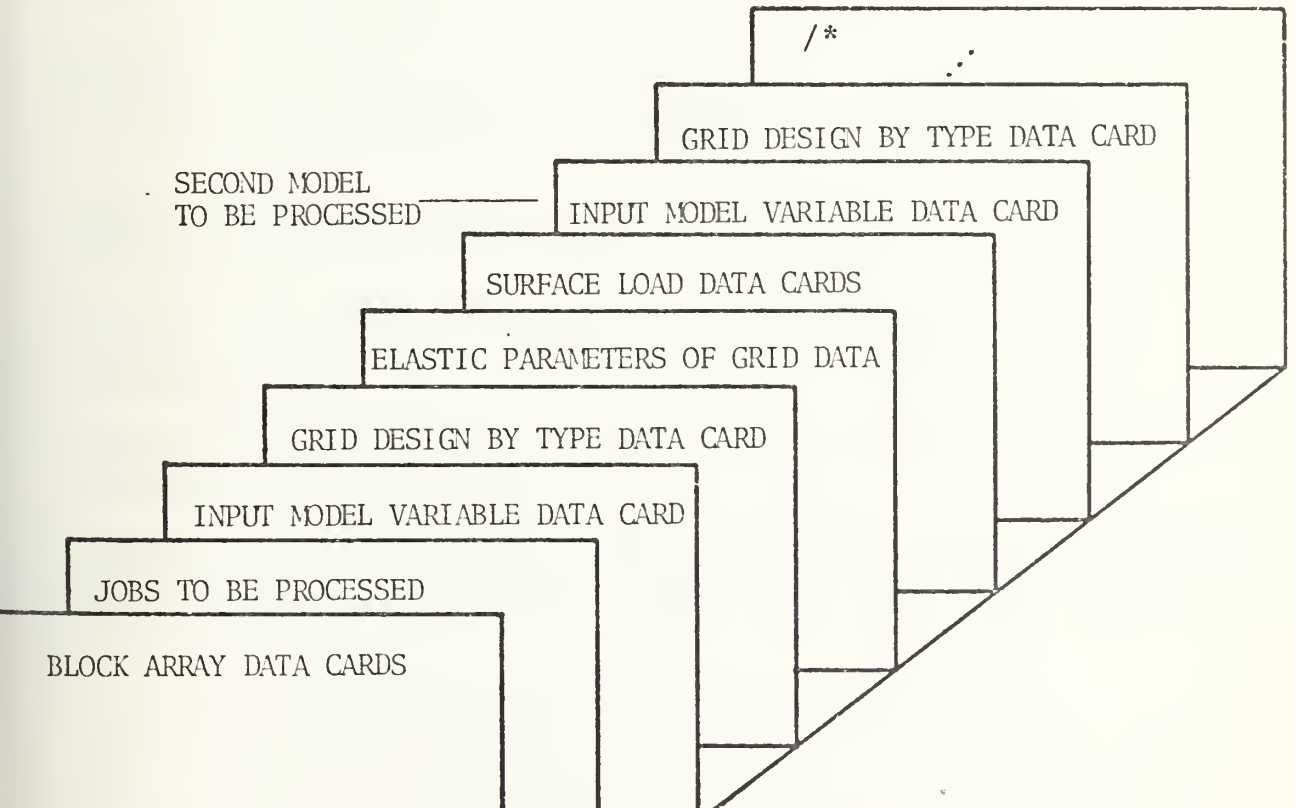
Young's overrelaxation method [5] was employed for solution of the equations. This is an iterative method used to improve the rate of convergence. The value of the overrelaxation parameter, W , must be specified with the input data. Because the optimum value of this parameter varies from problem to problem, efficient use of this method requires some experience. This inconvenience, however, is more than offset by the speed of this method and by the small amount of core which is required relative to simple and direct methods of solution. Other methods with comparable speed and storage place bothersome restrictions on the design and labeling of the finite element grid [3].

The subroutine QPLOT is a printer plot routine of the surface node displacements. It searches for the largest negative displacement and adds it to every nodal displacement. The plot then consists of all surface node displacements

plotted as a percent of the largest positive displacement. This was done to give the most clarity of detail possible to the plot. For each point on the plot, its associated surface node number and original displacements as calculated by subroutine ASAPS are printed.

Input Data Preparation

The first fifteen data cards of the data deck are called block array. They contain information about the construction of the grid from the five mesh types. These data cards are always required and always remain in the same position, regardless of the grid design. The following order of input data cards follows the block array data cards.



The above data cards in their proper formats are required to insure that the program will run successfully. The format for each parameter in the input data deck is described below.

Data Cards Supplied by Experimenter

Job Card

Columns	1	2
Format	I2	
Parameter	JOB	

Model Variables Data Card

Columns	1	4	5	9	10	14	15	19	20	24	25	29	30	34	35	39	40-44	45-46	47-48		
Format	I4		I5		I5		I5		I5		I5		I5		F5.3		I5		I5		I5
Parameter	IPO		NBLKS		NZ		NF		KBND		IGEOM		ITERAT		W		NA		NB		NC

Grid Design by Mesh Type Data Card

Columns	1	2	3	4	NBKS
Format	I1	I1	I1	I1	I1
Parameter	NBLK(1)	NBLK(2)	NBLK(3)	NBLK(4)	NBLK(NBKS)

Elastic Parameters of Grid Data Cards (There are NZ (Number) of These Data Cards)

Columns	1	5	6	10	11	15	16	20	21	27	28	34
Format	F5.1		F5.1		F5.1		F5.1		E7.1		E7.1	
Parameter	YZ1		YZ2		YZ1		YZ2		UZ1		UZ2	

Surface Loads Data Cards (There will be NF/10 (Rounded to Highest Whole Number) of these Data Cards)

Columns	1	5	6	10	11	15	16	20	21	25	26	30	31	35	36	40	41	45	46	50	
Format	F5.1		F5.1		F5.1		F5.1		F5.1		F5.1		F5.1		F5.1		F5.1		F5.1		F5.1
Parameter	FY		FY		FY		FY		FY		FY		FY		FY		FY		FY		FY

The input parameters are described as follows:

JOB specifies the total number of models to be processed in one run.

IPO print option of which there are eight. The printout is divided into four parts:

A cell numbers, locations of associated nodes and elastic parameters.

B node numbers and location and associated values of NDISP, DISP.

C node number and location and associated displacement.

D diagram of vertical displacements of surface nodes.

IPO = 1 prints A, B, C, D

IPO = 2 prints B, C, D

IPO = 3 prints A, only surface nodes B, C, D

IPO = 4 prints only surface nodes B, C, D

IPO = 5 prints only data associated with surface nodes in B and C, D

IPO = 6 prints C, D

IPO = 7 prints only data associated with surface nodes in C, D

IPO = 8 prints D.

NBLKS total number of mesh types used in grid design

NZ total number of elastic boundary conditions incorporated in grid design.

NF total number of surface nodes in grid design.

KBND code for boundary conditions of the grid:

0 all sides free

1 bottom rigid

2 sides rigid

3 bottom and sides rigid.

IGEOM code for plain strain or axisymmetric type of problem:

1 plain strain problem and stress strain calculations in ASAPS will be bypassed.

2 axisymmetric problem and stress strain calculations will be accomplished in ASAPS

ITERAT number of iterations taken for solution of simultaneous equations.

- W overrelaxation parameter used to reduce solution time and speed convergence. Value should be between 1.6 and 1.7.
- NA exponent of ten used as scale factor for nodal coordinates.
- NB exponent of ten used as scale factor for surface nodal forces.
- NC exponent of ten used as scale factor for nodal displacement (zero if cm. is required and cgs units are used for NA and NB)
- ND exponent of ten used as scale factor for elastic parameters (Lame's constants). If elastic parameters are loaded in exponential form, then ND = 0.
- NBLK subscripted variable containing coded quantity: of the grid design by mesh type.
- 1 course
 - 2 left link connector
 - 3 intermediate
 - 4 fine
 - 5 right link connector
- YZ1 Y coordinate of top left hand corner of boundary condition (in grid coordinates, i.e., inches)
- YZ2 Y coordinate of bottom left hand corner of boundary condition (in grid coordinates, i.e., inches)
- XZ1 X coordinate of top right hand corner of boundary condition (usually zero and also in grid coordinates, i.e., inches)
- XZ2 X coordinate of bottom right hand corner of boundary condition (in grid coordinates, i.e., inches).
- UZ1 Lamé constant Lamda (λ) coefficient of elasticity.
- UZ2 Lamé constant Mu (μ) coefficient of elasticity.
- FY(I) normal force at each of the surface nodes.

Example calculation for solving Lamé's constants given a velocity structure:

Find λ and μ for the sample velocity structure in the zone where $v_p = 6.0$ km/sec assuming Poisson ratio of .25.

$$\text{Poisson ratio } \sigma = \frac{\lambda}{2(\lambda + \mu)} \quad (1)$$

$$\text{Velocity for elastic waves (longitudinal waves, P waves)} v_p = \left(\frac{\lambda + 2\mu}{\rho} \right)^{1/2} \quad (2)$$

where ρ = density and is obtained from the Nafe-Drake curve which displays the variation of density with P wave velocity.

For $v_p = 6.0$ km/sec \longrightarrow $\rho = 2.75$ g/cm³

Now, solving equations 1 and 2 above simultaneously for λ and μ .

Equation 1

$$.25 = \frac{\lambda}{2(\lambda + \mu)}$$

$$.5 = \frac{\lambda}{\lambda + \mu}$$

$$.5\lambda + .5\mu = \lambda$$

$$\lambda = \lambda$$

Equation 2

$$6 \times 10^5 = \left(\frac{\lambda + 2\mu}{2.75} \right)^{1/2}$$

$$6 \times 10^5 = \left(\frac{3\lambda}{2.75} \right)^{1/2}$$

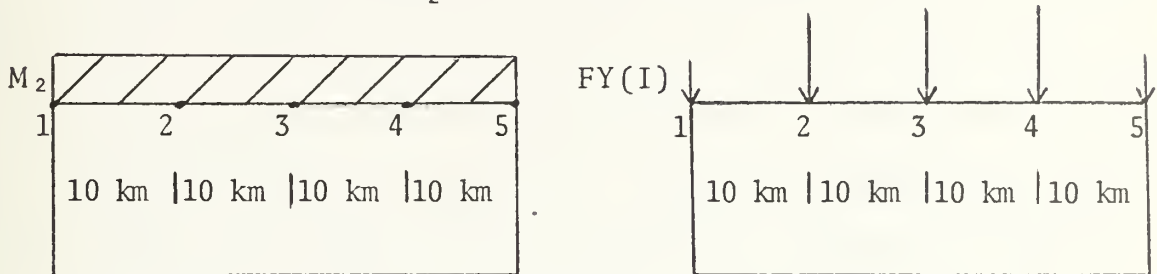
$$\lambda = 3.3 \times 10^{11}$$

$$\mu = 3.3 \times 10^{11} \text{ dynes/cm}^2$$

ANS.

Example calculation for determining scale factor (NB) and normal surface forces (FY) given the amplitude of the M_2 frequency of third tidal spectrum.

Find $FY(I)$, given $M_2 = 50$ centimeters?



$$\text{Force} = \text{Pressure} \cdot \text{Area}$$

$$\begin{aligned} \text{Pressure} &= \rho g h = 1 \text{ g/cm}^3 \times 9.8 \times 10^2 \text{ cm/sec}^2 \times 50 \text{ cm} \\ &= 4.9 \times 10^4 \end{aligned}$$

where ρ = density of sea water

g = gravity

h = amplitude of M_2

$$\begin{aligned} \text{Area} &= \text{Distance between nodes} \cdot 1 \text{ cm} \\ &= 10 \times 10^5 \text{ cm}^2 \end{aligned}$$

(Note: 1 cm is assumption of unit width of surface load.)

$$\text{Force} = 4.9 \times 10^4 \times 10 \times 10^5 = 49 \times 10^9 \text{ dynes at each interior node.}$$

$$\text{NB} = 9.$$

Nodes located at edges of load should be loaded with half as much force, to simulate a uniform load.

Derivation of NA for coordinate system in kilometers:

Let smallest mesh distance (.2 inches) equal 1 km.

$$\text{Then } .2 \text{ inches} = 1 \text{ km} = 1 \times 10^5 \text{ cm}$$

$$.5 \text{ inches} = 2.5 \text{ km} = 2.5 \times 10^5 \text{ cm.}$$

$$1 \text{ inch} = 5 \text{ km} = 5 \times 10^5 \text{ cm}$$

therefore $NA = 5$.

Core Requirements

Core requirements obviously depend upon the size of the grid (i.e., the total number of cells and nodes). Variables O, P, Q, XC, YC, AREN, ELAM, and EMU are subscripted in common with the total number of cells in the grid. Variables XF, YF, FX, FY, MID, LID, and LIDS are subscripted in common with the total number of nodes in the grid. Finally, variables A, AR, B, MAP, NDISP, and DISP are subscripted in common with twice the total number of nodes in the grid. A program with 744 cells and 419 nodes required 280 K bits of core on an IBM 360-67 computer. This was a very large grid spanning 74 modeling inches. For most grids of 500 cells or less, 200 K bits of core would be sufficient to run the program, on an IBM 360-67 computer. Of course, core requirements will differ from system to system. The above mentioned core requirements are meant to be a guide.

Time Requirements

The time required to run the finite element computer program is a function of the grid size, the number of iterations required to obtain a convergent solution and the amount of printout required. An IBM 360-67 computer required approximately fifteen minutes to process a 744 cell, 74 inch model grid using 1,000 iterations and a complete printout (IPO = 1). This time may be considerably reduced if only information about the surface displacements is required. Using IPO = 8 on the same grid and 1,000 iterations only eight minutes was

required to run the program. Again, if IPO = 8 is used on the same grid and only 300 iterations are required the program ran in four minutes. Of course, time requirements will differ depending on the system and the overhead required. The above mentioned time requirements are meant as a guide.

Internal Forces

Internal forces can be processed by this finite element computer program in conjunction with surface loads or instead of surface loads. However, each internal node force must be loaded manually into the program by inserting the appropriate instruction in the main program. The calculation of the size of the nodal force is the same as if it were a surface force. The sign of the force specified determines force direction. Positive force is a downward force and a negative force is an upward force. The internal force at node I should be loaded in the following format,

$$FY(I) = (\pm)(\text{force size}) * 10.** \text{ NB}$$

The internal force statements should be inserted between statement numbers FETO3590 and FETO3600 in the main program. If only internal forces are desired, blank data cards should be used in the input section for surface loads in the data deck.

Cutout Procedure

A problem faced by the experimenter is determination of a number of iterations sufficient to be assured that the solution has converged. This must be specified in the input data ITERAT. A number which far exceeds the point of

convergence wastes computer time and money. Therefore, in subroutine ASAPS variable CUT is specified in statement number FET04700. It is now arbitrarily set at 0.000001. CUT is compared with the percentage difference that some surface node has displaced in 25 iterations. Thus CUT is a percentage beyond which the experimenter feels the solution has converged and wishes to terminate the procedure. The surface node used for the comparison should be located either under the load system or in a zone where a large amount of deformation is expected to take place. The node number is determined by variable MIS specified in statement number FET04680 in the ASAPS subroutine. However, if the experimenter knows how many iterations are required and specifies that number in the input data, he may desire to by-pass the cutout procedure. This is accomplished by changing statement number FET06860 in ASAPS

```
from 901 IF(PERC.LE.CUT) GO TO 902  
to 901 IF(PERC.LE.CUT) GO TO 104.
```


Definitions of Non-Input Variables

DISP(I) displacement in x-direction of node I (cgs units)
DISP(I+NODE) displacement in y-direction of node I
FX(I) horizontal force at node I
NCELL total number of cells in grid
NDISP(I) = 1 displacement is set at 0.1, i.e., node I
is rigid in x-direction
= 0 displacement is unspecified at node I in
x-direction
NDISP(I+NODE) same as NDISP(I) except in y-direction
NODE total number of nodal points in grid
O(I) node number of uppermost left node in cell I
P(I) clockwise node number from O(I) in cell I
Q(I) clockwise node number from P(I) in cell I
XF(I) x coordinate of node I
YF(I) y coordinate of node I
AREN(I) area of cell I
IBL(I) the node number beginning layer I of the grid
(fine and intermediate have 9 layers
course has 7 layers)
IEL(I) the node number that ends layer I of the grid
CUT percentage change in the distance that some surface
node (determined by MIS) moves in 25 iterations.
(See cutout procedure)

LISTING OF FINITE ELEMENT TECHNIQUE COMPUTER PROGRAM

```

COMMON O(750),P(750),Q(750),XC(750,3),YC(750,3),ZC(750,3),
2XF(425),YF(425),FX(425),FY(425),NDISP(0850),DISP(0850),
3 XZ1(025),XZ2(025),YZ1(025),YZ2(025),UZ1(025),UZ2(025),
4A(850,16),AREN(750),AR(850),B(850),ELAM(750),EMU(750),
5LIDS(425,7),LID(425,8,2),MAP(850,16),MID(425,8),
6NA,NB,NC,ND,NODE,NCELL,IGEOM,ITERAT,W,NF,IPO
INTEGER O,P,Q,ON,PN,QN,OTEMP,CE,PE,QE
DIMENSION NBLK(50),BLK(5,5,10),LAY(10),IEL(10),IBL(10)

CF,YF,FX,FY,MID,LID,LIDS.....N TOTAL NUMBER NODES
O,P,Q,XC,YC,AREN,ELAM,EMU.....M TOTAL NUMBER CELS
A,AR,B,MAP,NDISP,DISP.....2N

CODE TYPE CELLS NODES L,R LNK
1 COARSE 25 20 7,7
2 L.LNK 14 16 7,7
3 INT 57 40 9,9
4 FINE 101 64 9,9
5 R.LNK 14 16 9,7

FORMAT(1X,'END DUE TO VARIABLE NBLKS EQUAL ZERO')
FORMAT(1X,'END DUE TO VARIABLE NZ EQUAL ZERO')
FORMAT(1X,'END DUE TO VARIABLE NF EQUAL ZERO')
FORMAT(2I5,6F5.1)
FORMAT(8F10.2)
FORMAT(2I5)
FORMAT(14,6I5,F5.3,4I5)
FORMAT(10F5.1)
FORMAT(50I1)
FORMAT(10X,7F10.2,2I5)
FORMAT(4F5.1,2E7.1)
FORMAT(15,4F10.2,2E10.2,15)
FORMAT(12)
FORMAT(10F5.1)
FORMAT(15,3E12.4,3(E12.4,I15))
FORMAT(1H1,50X,'BLK MATRIX (5,3,10) REMAINS CONSTANT',//)
FORMAT(10X,'DATA CARD',/,20X,'IPO NBLKS NZ NF KBND IGEOM ITERA
W NA NB NC ND NCELL NBLK NZ ND',/)
FORMAT(19X,I4,5I5,3X,I5,3X,F5.3,4I5,/)
FORMAT(1X,'AREA',6X,'XZ1',7X,'XZ2',7X,'YZ1',7X,'YZ2',7X,'UZ1',7X,
1,UZ2',2X,'ARLA',/)
FORMAT(1H1,3X,4HCELL,1X,'O X-COORD',3X,'O Y-COORD',3X,
1,P X-COORD',3X,'P Y-COORD',3X,'Q X-COORD',3X,'Q Y-COORD',4X,1H0,4X
2,1HP,4X,1HQ,6X,5HLAMDA,6X,2HMU,4X,4HCELL)
FORMAT(1H1,1X,4HNODE,3X,7HX-COORD,5X,7HY-COORD,3X,6HXFORCE,9X,

```



```

16HYFORCE,4X,6HNDISPX,1X,5HDISPY,1X,6HNDISPY,4X,4HNDDE,
23X,NOTE COORD IN CGS UNITS',//)
903 FORMAT(I5,6E12.4,3I5,2E12.4,15)
904 FORMAT(I5,8F10.2)
905 FORMAT(4I5,6F10.2)
9033 FORMAT(1X,15,6E12.4,3I5,2X,2E10.2,2X,I3)
9034 WRITE(6,720)
C      DO 59 I=1,5
C      DO 59 J=1,3
C      READ(5,104) (BLK(I,J,K),K=1,10)
C      WRITE(6,104) (BLK(I,J,K),K=1,10)
C      59 CONTINUE
C
C      INPUT CARD*****JOB=NUMBER OF MODELS TO BE PRECESSED
C      THIS CARD PRECEDES DATA FOR MODELS (FORMATI2)
C
C      READ(5,666) JOB
C      DO 1000 NNK=1,JOB,1
C
C      INPUT CARD
C      IPO=OUTPUT PRINT OPTION PRINT OUT IS IN FOUR PARTS
C      A=CELLNUMBERS, LOCATION OF ASSOCIATED NODES, LAMDA, MU
C      B=NODES AND THEIR ASSOCIATED LOCATION, NDISP, DISP
C      C=DISPLACEMENTS IN X AND Y DIRECTION OF NODES
C      D=PRINTER PLOT OF SURFACE NODES
C      IPO=1 PRINTS A,B,C,D
C      IPO=2 PRINTS B,C,D
C      IPO=3 PRINTS A, ONLY SURFACE NODES IN B,C,D
C      IPO=4 PRINTS A, ONLY SURFACE NODES IN B,C,D
C      IPO=5 PRINTS ONLY DATA ASSOCIATED WITH SURFACE NODES IN B AND C,D
C      IPO=6 PRINTS C,D
C      IPO=7 PRINTS C,D
C      IPO=8 PRINTS ONLY D
C      NBKKS=TOTAL NUMBER OF MESH TYPES USED IN GRID CONSTRUCTION
C      NZ=NUMBER ELASTIC BOUNDARY FIELDS.
C      NF=NUMBER SURFACE NODES.
C      KRND=0 ALL SIDES FREE (1) BOTTOM FIXED (2) SIDES FIXED (3) BOTTO
C      AND SIDES FIXED
C      ICEOM=1 IF STRESS-STRAIN CALCULATIONS IN SUBROUTINE ASAPS ARE TO
C      BE BYPASSED. OTHERWISE ICEOM CAN BE ANY OTHER INTEGER.
C      ITERAT=NUMBER ITERATIONS TAKEN FOR SOLUTION OF SIMULTANEOUS
C      EQUATIONS IN SUBROUTINE ASAPS.
C      NA,NB,NC,ND=EXONENT OF TEN USED AS SCALE FACTORS
C      NA--X,MY,XF,YF(DIMENSIONS OF MESH, COORDINATES OF NODES)
C      NB--FY (NORMAL FORCE)
C      NC SCALE FACTOR FOR DISPLACEMENTS
C      ND--ELAM, EMU (ELASTIC PARAMETERS)
C      W OVERRELAXATION PARAMETER 1.6<W<1.7

```



```

WRITE(6,721) IPO,NBLKS,NZ,NF,K6ND,IGEOM,ITERAT,W,NA,NB,NC,ND
WRITE(5,103) IPO,NBLKS,NZ,NF,K6ND,IGEOM,ITERAT,W,NA,NB,NC,ND
WRITE(6,722) IPO,NBLKS,NZ,NF,K6ND,IGEOM,ITERAT,W,NA,NB,NC,ND
IF (NBLKS.EQ.0) GO TO 1111
INPUT CARD
NBLK(I)=TYPE OF I(TH) SECTION OF MESH, READING FROM LEFT TO RIGHT.
IE., SEQUENCE OF COARSE, L.LNK,INT., FINE, R.LNK IS READ IN AS 123
READ(5,105) (NBLK (I), I=1,NBLKS)
X=0.
Y=0.
K=0
IBLK1=NBLK(1)
XMX=0
YMX=12.
DU 50 KN=1,NBLKS
I=NBLK (KN)
Y=0
X=XMX
XX=BLK(I,1,10)
XMX=XMX+XX
IF(KN.EQ.1) X=0
DO 51 J=1,9
IC=BLK(I,3,J)
IF(IC.EQ.0) GO TO 50
YV=BLK(I,2,J)
WRITE (6,905) KN,J,K,IC,X,Y,XV,YV,XMX,XX
GO TO (501,502,503,504),IC
CONTINUE
XVV=XV
IF (IC.EQ.2.OR.IC.EQ.5) XVV=2.*XV
IF(X+XVV-XMX) 511,513,513
X=X+XVV
Y=Y+YV
IF(Y-YMX) 52,50,50
X=XMX-XX
GO TO 51
K=K+1
XC(K,1)=X
YC(K,1)=Y
XC(K,2)=X+XV
YC(K,2)=Y
XC(K,3)=X
YC(K,3)=Y+YV
K=K+1
XC(K,1)=X+XV
YC(K,1)=Y

```

```

FET00960
FET00970
FET00980
FET00990
FET01000
FET01010
FET01020
FET01030
FET01040
FET01050
FET01060
FET01070
FET01080
FET01090
FET01100
FET01110
FET01120
FET01130
FET01140
FET01150
FET01160
FET01170
FET01180
FET01190
FET01200
FET01210
FET01220
FET01230
FET01240
FET01250
FET01260
FET01270
FET01280
FET01290
FET01300
FET01310
FET01320
FET01330
FET01340
FET01350
FET01360
FET01370
FET01380
FET01390
FET01400
FET01410
FET01420
FET01430
FET01440
FET01450

```

```

C
C
C
C
C

```

```

C

```

```

1009
511
513
52
501

```


FET01460
 FET01470
 FET01480
 FET01490
 FET01500
 FET01510
 FET01520
 FET01530
 FET01540
 FET01550
 FET01560
 FET01570
 FET01580
 FET01590
 FET01600
 FET01610
 FET01620
 FET01630
 FET01640
 FET01650
 FET01660
 FET01670
 FET01680
 FET01690
 FET01700
 FET01710
 FET01720
 FET01730
 FET01740
 FET01750
 FET01760
 FET01770
 FET01780
 FET01790
 FET01800
 FET01810
 FET01820
 FET01830
 FET01840
 FET01850
 FET01860
 FET01870
 FET01880
 FET01890
 FET01900
 FET01910
 FET01920
 FET01930
 FET01940
 FET01950

502 XC(K, 2)=X+XV
 YC(K, 2)=Y+YV
 XC(K, 3)=X
 YC(K, 3)=Y+YV
 GO TO 1009
 CONTINUE
 K=K+1
 XC(K, 1)=X
 YC(K, 1)=Y
 XC(K, 2)=X+XV
 YC(K, 2)=Y
 XC(K, 3)=X
 YC(K, 3)=Y+YV
 K=K+1
 XC(K, 1)=X+XV
 YC(K, 1)=Y
 XC(K, 2)=X+2*XV
 YC(K, 2)=Y+YV
 XC(K, 3)=X
 YC(K, 3)=Y+YV
 K=K+1
 XC(K, 1)=X+XV
 YC(K, 1)=Y
 XC(K, 2)=X+2*XV
 YC(K, 2)=Y
 XC(K, 3)=X+2*XV
 YC(K, 3)=Y+YV
 GO TO 1009
 CONTINUE
 503 K=K+1
 XC(K, 1)=X
 YC(K, 1)=Y
 XC(K, 2)=X+XV
 YC(K, 2)=Y
 XC(K, 3)=X+XV
 YC(K, 3)=Y+YV/2.
 K=K+1
 XC(K, 1)=X
 YC(K, 1)=Y
 XC(K, 2)=X+XV
 YC(K, 2)=Y+YV/2
 XC(K, 3)=X
 YC(K, 3)=Y+YV
 K=K+1
 XC(K, 1)=X+XV
 YC(K, 1)=Y+YV/2.
 XC(K, 2)=X+XV
 YC(K, 2)=Y+YV
 XC(K, 3)=X
 YC(K, 3)=Y+YV

FET01960
 FET01970
 FET01980
 FET01990
 FET02000
 FET02010
 FET02020
 FET02030
 FET02040
 FET02050
 FET02060
 FET02070
 FET02080
 FET02090
 FET02100
 FET02110
 FET02120
 FET02130
 FET02140
 FET02150
 FET02160
 FET02170
 FET02180
 FET02190
 FET02200
 FET02210
 FET02220
 FET02230
 FET02240
 FET02250
 FET02260
 FET02270
 FET02280
 FET02290
 FET02300
 FET02310
 FET02320
 FET02330
 FET02340
 FET02350
 FET02360
 FET02370
 FET02380
 FET02390
 FET02400
 FET02410
 FET02420
 FET02430
 FET02440
 FET02450

504 GO TO 1009
 CONTINUE
 K=K+1
 XC(K,1)=X
 XC(K,2)=X+XV
 XC(K,3)=Y
 XC(K,4)=Y+YV/2.
 K=K+1
 XC(K,1)=X+XV
 XC(K,2)=Y
 XC(K,3)=X+XV
 XC(K,4)=Y+YV
 XC(K,5)=X
 XC(K,6)=Y+YV/2.
 K=K+1
 XC(K,1)=X
 XC(K,2)=Y+YV/2.
 XC(K,3)=X+XV
 XC(K,4)=Y+YV
 XC(K,5)=X
 XC(K,6)=Y+YV
 GO TO 1009
 CONTINUE
 51 CONTINUE
 50

C
 C
 C
 FIND AND REPLACE (REDUCE) ALL COMMON NODES TO LOWEST ORDER

J1=0
 K7=0
 DY=0.2
 DX=0.5
 K6=0
 X=0
 Y=0
 YMX=12.2
 XMX=0
 DO 969 N=1,NBLKS
 KN=NBLK(N)
 XMX=XMX+BLK(KN,1,10)
 XMX=(5.*XMX)*10.**NA
 YMX=(5.*YMX)*10.**NA
 NYI=2+YMX
 NXI=1+XMX/DX
 DO 950 I=1,NYI
 DO 951 I=1,NXI
 K7=0
 IH=0
 DO 953 I=1,K


```

FET02460
FET02470
FET02480
FET02490
FET02500
FET02510
FET02520
FET02530
FET02540
FET02550
FET02560
FET02570
FET02580
FET02590
FET02600
FET02610
FET02620
FET02630
FET02640
FET02650
FET02660
FET02670
FET02680
FET02690
FET02700
FET02710
FET02720
FET02730
FET02740
FET02750
FET02760
FET02770
FET02780
FET02790
FET02800
FET02810
FET02820
FET02830
FET02840
FET02850
FET02860
FET02870
FET02880
FET02890
FET02900
FET02910
FET02920
FET02930
FET02940
FET02950

```

```

DO 955 L=1,3
IF(XC(I,L).GE.X.AND.XC(I,L).LT.X+DX.AND.
C YC(I,L).GE.Y.AND.YC(I,L).LT.Y+DY)GO TO 952
GO TO 955
952 K7=K7+1
IF(IH.EQ.0)J1=J1+1
JT=J1
IH=I
GO TO (1,2,3),L
1 O(I)=JT
GO TO 954
2 P(I)=JT
GO TO 954
3 Q(I)=JT
954 CONTINUE
955 GO TO 953
953 CONTINUE
951 X=X+DX
CONTINUE
X=0
Y=Y+DY
DY=1
CONTINUE
950 CONTINUE
959 DO 909 J=1,K
WRITE(6,903) J,XC(J,1),YC(J,2),XC(J,2),YC(J,3),
C XC(J,3),YC(J,3)
909 CONTINUE
NCELL=K
IF(O(K).GE.P(K).AND.O(K).GE.Q(K)) NCDE=O(K)
IF(P(K).GE.O(K).AND.P(K).GE.Q(K)) NCDE=P(K)
IF(Q(K).GE.O(K).AND.Q(K).GE.P(K)) NCDE=Q(K)
DO 703 J=1,K
I=O(J)
XF(I)=(5.*XC(J,1))*10.**NA
YF(I)=(5.*YC(J,1))*10.**NA
I=P(J)
XF(I)=(5.*XC(J,2))*10.**NA
YF(I)=(5.*YC(J,2))*10.**NA
I=Q(J)
XF(I)=(5.*XC(J,3))*10.**NA
YF(I)=(5.*YC(J,3))*10.**NA
CONTINUE
703 IF(NZ.EQ.0) GO TO 1112
WRITE(6,723)
DO 20 N=1,NZ
C INPUT CARDS
C ELASTIC BOUNDARY FIELDS MAY OVERLAP I.E. ARE INDEPENDENT OF MESH

```


C LATTER BOUNDARY CONTIONS TAKE PRECEDENCE OVER FORMER BOUNDARIES
 C NOTE REVERSE READ Y1,Y2 THEN X1,X2...ETC IN READ(5,605)
 C XZ1,YZ1=X,Y COORDINATES OF TOP LEFT-HAND CCRNER OF BOUNDARY
 C XZ2=X COORDINATE OF RIGHT-HAND BOUNDARY.
 C YZ2=Y COORDINATE OF BOTTOM BOUNDARY.
 C UZ1,UZ2=LAMBDA,MU,RESPECTIVELY.

20 READ(5,605) YZ1(N),YZ2(N),XZ1(N),XZ2(N),UZ1(N),UZ2(N)
 WRITE(6,606)N,XZ1(N),XZ2(N),YZ1(N),YZ2(N),UZ1(N),UZ2(N),N
 CONTINUE

106 JJ=1
 KCC=0
 DO 112 N=1,NBLKS,1
 KN=NBLK(N)
 GO TO(106,107,108,109,107),KN

107 KC=23
 GO TO 110
 KC=14
 GO TO 110
 108 KC=57
 GO TO 110
 109 KCC=KCC+KC
 110 DO 801 I=1,NZ,1
 DO 111 J=JJ,KCC,1

E=XZ1(I)
 F=XZ2(I)
 G=YZ1(I)
 H=YZ2(I)
 IF(XC(J,I)).LT.E.OR.XC(J,2).LT.E.OR.XC(J,3).LT.E.OR.
 XC(J,I).GT.F.OR.XC(J,2).GT.F.OR.XC(J,3).GT.F) GO TO 111
 IF(YC(J,I)).LT.G.OR.YC(J,2).LT.G.OR.YC(J,3).LT.G.OR.
 YC(J,I).GT.H.OR.YC(J,2).GT.H.OR.YC(J,3).GT.H) GO TO 111
 ELAM(J)=UZ1(I)*10.**ND
 EMU(J)=UZ2(I)*10.**ND

111 CONTINUE
 801 CONTINUE
 112 JJ=JJ+KC
 CONTINUE
 IF(IPO.GE.3)GO TO 113
 WRITE(6,724)
 WRITE(6,9034)
 DO 113 J=1,K,1

907 WRITE(6,9033) J,XC(J,1),YC(J,1),XC(J,2),YC(J,2),XC(J,3),YC(J,3),
 20 CONTINUE
 113 IF (NF.EQ.0) GO TO 1113

C INPUT CARDS

FET02960
 FET02970
 FET02980
 FET02990
 FET03000
 FET03010
 FET03020
 FET03030
 FET03040
 FET03050
 FET03060
 FET03070
 FET03080
 FET03090
 FET03100
 FET03110
 FET03120
 FET03130
 FET03140
 FET03150
 FET03160
 FET03170
 FET03180
 FET03190
 FET03200
 FET03210
 FET03220
 FET03230
 FET03240
 FET03250
 FET03260
 FET03270
 FET03280
 FET03290
 FET03300
 FET03310
 FET03320
 FET03330
 FET03340
 FET03350
 FET03360
 FET03370
 FET03380
 FET03390
 FET03400
 FET03410
 FET03420
 FET03430
 FET03440
 FET03450

FET 03460
 FET 03470
 FET 03480
 FET 03490
 FET 03500
 FET 03510
 FET 03520
 FET 03530
 FET 03540
 FET 03550
 FET 03560
 FET 03570
 FET 03580
 FET 03590
 FET 03600
 FET 03610
 FET 03620
 FET 03630
 FET 03640
 FET 03650
 FET 03660
 FET 03670
 FET 03680
 FET 03690
 FET 03700
 FET 03710
 FET 03720
 FET 03730
 FET 03740
 FET 03750
 FET 03760
 FET 03770
 FET 03780
 FET 03790
 FET 03800
 FET 03810
 FET 03820
 FET 03830
 FET 03840
 FET 03850
 FET 03860
 FET 03870
 FET 03880
 FET 03890
 FET 03900
 FET 03910
 FET 03920
 FET 03930
 FET 03940
 FET 03950

```

C
C
FY=NORMAL FORCE.
READ(5,707) (FY(I),I=1,NF)
DO 705 I=1,NCDE
  FX(I)=0
  IF(I+NF.GT.NCDE) GO TO 5555
  FY(I+NF) = 0
  CONTINUE
  FY(I)=FY(I)*10.**NB
  NDISP(I)=0
  NDISP(I+NCDE)=0
  DISP(I)=1
  DISP(I+NCDE)=1
  CONTINUE
  IF(K6ND.EQ.0)GO TO 4445
  DO 60 J=1,9,1
    NBL=1
    IF(J.EQ.4.OR.J.EQ.6.OR.J.GE.8) GO TO 61
    IF(J.EQ.7) NBL=2
    LAY(J)=1,NBLKS,1
    K=NBLK(N)
    GO TO(63,64,65,66,64,66),K
    LAY(J)=LAY(J)+2
    GO TO 62
  LAY(J)=LAY(J)+1
  GO TO 62
  LAY(J)=LAY(J)+4
  GO TO 62
  LAY(J)=LAY(J)+8/NBL
  CONTINUE
  GO TO 60
  IF(J.GE.8)GO TO 67
  LAY(J)=0
  DO 68 N=1,NBLKS,1
    K=NBLK(N)
    GO TO(68,69,70,71,68,71),K
    LAY(J)=LAY(J)+1
    GO TO 68
  LAY(J)=LAY(J)+4
  GO TO 68
  LAY(J)=LAY(J)+8
  CONTINUE
  GO TO 60
  IF(J.EQ.9)GO TO 72
  LAY(J)=1
  DO 73 N=1,NBLKS,1
    K=NBLK(N)
    GO TO(74,75,74,74,75,74),K
    LAY(J)=LAY(J)+2
  
```

5555

705

63

64

65

66

62

61

69

70

71

68

67

74

FET03960
 FET03970
 FET03980
 FET03990
 FET04000
 FET04010
 FET04020
 FET04030
 FET04040
 FET04050
 FET04060
 FET04070
 FET04080
 FET04090
 FET04100
 FET04110
 FET04120
 FET04130
 FET04140
 FET04150
 FET04160
 FET04170
 FET04180
 FET04190
 FET04200
 FET04210
 FET04220
 FET04230
 FET04240
 FET04250
 FET04260
 FET04270
 FET04280
 FET04290
 FET04300
 FET04310
 FET04320
 FET04330
 FET04340
 FET04350
 FET04360
 FET04370
 FET04380
 FET04390
 FET04400
 FET04410
 FET04420

```

75 GO TO 73
73 LAY(J)=LAY(J)+1
   CONTINUE
72 GO TO 60
60 LAY(J)=NBLKS+1
   CONTINUE
   IBL(I)=1
   DO 76 J=2,9,1
     IBL(J)=IBL(J-1)+1
     IEL(J)=IEL(J-1)+LAY(J)
76 CONTINUE
   IF(KBND.EQ.2) GO TO 4446
   KBL=IBL(9)
   KEL=IEL(9)
   DO 4444 I=KBL,KEL,1
     NDISP(I)=1
     NDISP(I+NODE)=1
4444 CONTINUE
   IF(KBND.EQ.1) GO TO 4445
4446 DO 4445 I=1,8,1
     IF(I.EQ.4)OK,I=EQ.6)GO TO 4445
     NDISP(IBL(I))=1
     NDISP(IEI(I))=1
     NDISP(IEI(I)+NOD)=1
     NDISP(IEI(I)+NOD)=1
4445 CONTINUE
     NOD=0
     IF(IPO.GE.6) GO TO 440
     IF(IPO.EQ.1)OR.IPO.EQ.2)NOD=NODE
     IF(IPO.GE.3)AND.IPO.LE.5)NOD=NF
     WRITE(6,725)
80 DO 708 I=1,NOD,1
     WRITE(6,709) I,XF(I),YF(I),FX(I),FY(I),NDISP(I),DISP(I),
2     NDISP(I+NODE),DISP(I+NODE),I
440 CONTINUE
708 CONTINUE
1000 CALL ASAPS(JOB)
CONTINUE
GO TO 14
1111 WRITE(6,11)
1112 GO TO 14
1112 WRITE(6,12)
GO TO 14
1113 WRITE(6,13)
14 STOP
END

```


FET04940
 FET04950
 FET04960
 FET04970
 FET04980
 FET04990
 FET05000
 FET05010
 FET05020
 FET05030
 FET05040
 FET05050
 FET05060
 FET05070
 FET05080
 FET05090
 FET05100
 FET05110
 FET05120
 FET05130
 FET05140
 FET05150
 FET05160
 FET05170
 FET05180
 FET05190
 FET05200
 FET05210
 FET05220
 FET05230
 FET05240
 FET05250
 FET05260
 FET05270
 FET05280
 FET05290
 FET05300
 FET05310
 FET05320
 FET05330
 FET05340
 FET05350
 FET05360
 FET05370
 FET05380
 FET05390
 FET05400
 FET05410
 FET05420
 FET05430

```

C C
  LID(I,J,K)=CELLS WITH NODE PAIR I,L...L=MID(I,J),K=1-2
  DO 60 I=1,NODE,I
    MID(I,I)=I
  CONTINUE
  DO 61 I=1,NCELL,I
    ON=O(I)
    PN=P(I)
    CN=Q(I)
    DO 62 IC=1,3,I
      IF(IC.EQ.1) JT=ON
      IF(IC.EQ.2) JT=PN
      IF(IC.EQ.3) JT=QN
    DO 55 J=1,7,I
      IF(LIDS(JT,J).EQ.0) GO TO 63
  CONTINUE
  WRITE(6,833)JT
  WRITE(6,834)
  WRITE(6,835)(LIDS(JT,IE),IE=1,7,1),I
  STOP
  FORMAT(3X,39HERROR...TOO MANY CELLS ADJACENT TO NODE,I3)
  833 FORMAT(3X,26HCELLS ADJACENT TO THE NODE)
  834 FORMAT(3X,8I6)
  63 LIDS(JI,J)=I
  J=J+1
  CONTINUE
  DO 64 ITP=1,3,I
    DO 73 J=2,8,I
      IF(MID(ON,J).EQ.0) GO TO 66
      IF(MID(ON,J).EQ.PN ) GO TO 67
  CONTINUE
  J=J+1
  DO 74 J=2,8,I
    IF(MID(ON,J).EQ.0) GO TO 68
    IF(MID(ON,J).EQ.QN ) GO TO 69
  CONTINUE
  IF(J.EQ.9) WRITE(6,850) ON,(MID(ON,K),K=2,8,1),QN
  IF(J.EQ.9) STOP
  850 FORMAT(2X,20HERROR IN DATA, NODE ,I3,2X,20HADJACENT TO NODES
  15)
  68 MID(ON,J)=QN
  J=J+1
  69 OTEMP=ON
  CN=PN
  PN=QN
  CN=OTEMP
  CONTINUE
  64 CONTINUE
  61 DO 70 I=1,NODE,I

```

, 81

FET 05440
 FET 05450
 FET 05460
 FET 05470
 FET 05480
 FET 05490
 FET 05500
 FET 05510
 FET 05520
 FET 05530
 FET 05540
 FET 05550
 FET 05560
 FET 05570
 FET 05580
 FET 05590
 FET 05600
 FET 05610
 FET 05620
 FET 05630
 FET 05640
 FET 05650
 FET 05660
 FET 05670
 FET 05680
 FET 05690
 FET 05700
 FET 05710
 FET 05720
 FET 05730
 FET 05740
 FET 05750
 FET 05760
 FET 05770
 FET 05780
 FET 05790
 FET 05800
 FET 05810
 FET 05820
 FET 05830
 FET 05840
 FET 05850
 FET 05860
 FET 05870
 FET 05880
 FET 05890
 FET 05900
 FET 05910
 FET 05920
 FET 05930

```

DC 71 J=2,8,1
LTEMP=MID(I,J)
IF(LTEMP.EQ.0)GO TO 70
CO 72 K=1,7,1
KTEMP=LIDS(I,K)
IF(KTEMP.EQ.0) GO TO 71
ON=0(KTEMP)
PN=P(KTEMP)
GN=Q(KTEMP)
M=1
IF(LID(I,J,M).NE.0) M=2
IF(ON.EQ.LTEMP.OR.PN.EQ.LTEMP.OR.QN.EQ.LTEMP)LID(I,J,M)=KTEMP
CONTINUE
CONTINUE
CONTINUE
LET A(I,J)=0,MAP(I,J)=0,B(I)=0
DO 77 I = 1, IT, 1
DO 78 J = 1, 10, 1
A(I,J)=0
NAP(I,J)=0
CONTINUE
B(I)=0
CONTINUE
ITERATION ON I=NCCELL IS TO FORM YC(..),XC(..)
DO 85 I = 1, NCELL, 1
GN=0(I)
PN=P(I)
QN=Q(I)
YC(I,1)=Y(PN)-Y(QN)
YC(I,2)=Y(QN)-Y(ON)
YC(I,3)=Y(ON)-Y(PN)
XC(I,1)=X(QN)-X(PN)
XC(I,2)=X(ON)-X(QN)
XC(I,3)=X(PN)-X(ON)
AREN(I)=.5*(XC(I,1)*YC(I,3)-XC(I,3)*YC(I,1))
CONTINUE
*****
* FORM STIFFNESS MATRIX *
*****
DO 90 I=1,NODE,1
IV=NODE+I
DO 91 JA=1,8,1
J=MID(I,JA)
JB=JA+8
LD=0
DO 92 KA=1,7,1
LD=LD+1
IF(I.EQ.J) GO TO 94

```

72
 71
 70

78
 77

85

C
 C
 C
 C
 C

FET05940
 FET05950
 FET05960
 FET05970
 FET05980
 FET05990
 FET06000
 FET06010
 FET06020
 FET06030
 FET06040
 FET06050
 FET06060
 FET06070
 FET06080
 FET06090
 FET06100
 FET06110
 FET06120
 FET06130
 FET06140
 FET06150
 FET06160
 FET06170
 FET06180
 FET06190
 FET06200
 FET06210
 FET06220
 FET06230
 FET06240
 FET06250
 FET06260
 FET06270
 FET06280
 FET06290
 FET06300
 FET06310
 FET06320
 FET06330
 FET06340
 FET06350
 FET06360
 FET06370
 FET06380
 FET06390
 FET06400
 FET06410
 FET06420
 FET06430

```

IF(LD.GT.2) GO TO 92
K=LID(I,JA,KA)
GO TO 95
K=LIDS(I,KA)
94 IF(K.EQ.0) GO TO 92
95 AREA=ABS(AREN(K))
IH=I
DO 97 IL=1,2,1
IF(G(K).EQ.IH) KJ=1
IF(P(K).EQ.IH) KJ=2
IF(Q(K).EQ.IH) KJ=3
YJ=YC(K,KJ)
XJ=XC(K,KJ)
IF(IL.EQ.2) GO TO 97
IH=J
XI=XJ
YI=YJ
CONTINUE
AT1=(2.**XJ* ELAM(K))+XI*XJ* EMU(K))/(4.*AREA)
AT2=(YI*XJ* ELAM(K))+YI*XJ* EMU(K))/(4.*AREA)
AT3=(XI*XJ* ELAM(K))+YI*XJ* EMU(K))/(4.*AREA)
AT4=(2.**XI*XJ*(.5* ELAM(K))+ ELAM(K))/(4.*AREA)
IF(IGECM.EQ.1) GO TO 98
C
C
C ADDITIONS TO MATRIX FOR AXI-SYMMETRIC
CN=Q(K)
PN=P(K)
CN=Q(K)
XAV=(X(CN)+X(PN)+X(QN))/3.
AT1=(AT1*3.1416*2.**XAV)+(4.16*AREA/9.**XAV)*(EMU(K)+
1 5*ELAM(K))+((AREA*3.1416*ELAM(K))*(YI+YJ))/(3.**AREN(K))
AT2=(AT2*3.1416*2.**XAV)+(3.1416*AREA*ELAM(K)*XJ)/(3.**AREN(K))
AT3=(AT3*3.1416*2.**XAV)+(3.1416*AREA*ELAM(K)*XI)/(3.**AREN(K))
AT4=AT4*3.1416*2.**XAV
98 A(I,JA)=A(I,JA)+AT1
A(I,JB)=A(I,JB)+AT2
A(IV,JA)=A(IV,JA)+AT3
A(IV,JB)=A(IV,JB)+AT4
92 CONTINUE
MAP(I,JA)=J+NODE
MAP(I,JB)=J+NODE
MAP(IV,JA)=J
MAP(IV,JB)=J+NODE
91 CONTINUE
90 CONTINUE

```

 * ADD SPECIFIED LOADS TO B(I) *

C
 C
 C

C
 C
 C
 C


```

C      DO 100 I=1,NCODE,1
      IV=NODE+I
      B(I)=FX(I)
      B(IV)=FY(I)
      CCNTINUE
C      ARRANGE MATRIX FOR SOLUTION
      DO 101 I=1,IT,1
      DO 102 J=1,16,1
      IF (I.EQ.MAP(I,J)) GO TO 103
      CONTINUE
      AR(I)=A(I,J)
      CONTINUE
C      SOLVE SIMULTANEOUS EQUATIONS
      M=0
      DO 104 L=1,ITERAT,1
      DO 105 I=1,IT,1
      IF (NDISP(I).EQ.1) GO TO 105
      TEMP=0.
      DO 106 J=1,16,1
      IF (MAP(I,J).EQ.0) GO TO 106
      IF (I.EQ.MAP(I,J)) GO TO 106
      JROW=MAP(I,J)
      TEMP=TEMP+A(I,J)*DISP(JROW)
      CONTINUE
      DISP(I) = ((B(I) - TEMP)/AR(I))*W+((1.-W)*DISP(I))*10.**NC
      IF (DISP(I).GT.1.0E07) GO TO 825
      CONTINUE
      IF (L.NE.25.AND.L.LE.49) GO TO 104
      ITL=L/25
      IF (ITL.NE.L) GO TO 901
      M=M+1
      GO TO (15,16,2001),M
      DIST(M)=SQRT((DISP(MIS))**2+(DISP(MIDD))**2)
      GO TO 104
      DIST(N)=SQRT((DISP(MIS))**2+(DISP(MIDD))**2)
      PERC=SQRT((DIST(M-1)-DIST(M))**2)/DIST(M-1)
      DIST(M-1)=DIST(M)
      M=M-1
      IF (PERC.LE.CUT) GO TO 902
      CONTINUE
      M=2
      WRITE(6,163) L
      IF (IPO.EQ.8) GO TO 2
      WRITE(6,110)
      WRITE(6,111)
      NOD=NODE
      2
906
15
16
901 104
902
904

```

```

FET 06440
FET 06450
FET 06460
FET 06470
FET 06480
FET 06490
FET 06500
FET 06510
FET 06520
FET 06530
FET 06540
FET 06550
FET 06560
FET 06570
FET 06580
FET 06590
FET 06600
FET 06610
FET 06620
FET 06630
FET 06640
FET 06650
FET 06660
FET 06670
FET 06680
FET 06690
FET 06700
FET 06710
FET 06720
FET 06730
FET 06740
FET 06750
FET 06760
FET 06770
FET 06780
FET 06790
FET 06800
FET 06810
FET 06820
FET 06830
FET 06840
FET 06850
FET 06860
FET 06870
FET 06880
FET 06890
FET 06900
FET 06910
FET 06920
FET 06930

```



```

VP=DISP(PE)
VQ=DISP(QE)
EX={UO*YC(I,1)+UP*YC(I,2)+UQ*YC(I,3)}/(2.*AREN(I))
EY={VO*XC(I,1)+VP*XC(I,2)+VQ*XC(I,3)}/(2.*AREN(I))
EY=(JO*XC(I,1)+UP*XC(I,2)+UQ*XC(I,3)+VO*YC(I,1)+VP*YC(I,2)+VQ*YC(I,3))/
(4.*AREN(I))
AE=EX-EY
BE=EX+EY
AEP=ABS(AE)
IF(AEP.LT.00001) GO TO 201
EBETA=ATAN(2.*EXY)/AE)/2.
GO TO 202
EBETA=3.14159/4.
EGAM=EBETA+3.14159/2.
EPI=(BE/2.)+(AE/2.)*COS(2.*EBETA)+EXY*SIN(2.*EBETA)
EP2=(BE/2.)+(AE/2.)*COS(2.*EGAM)+EXY*SIN(2.*EGAM)
IF(EPI.LT.EP2) GO TO 203
EMAX=EPI
EMIN=EP2
THETA1=EBETA
THETA2=EGAM
GO TO 204
EMAX=EPI
EMIN=EP2
THETA1=EGAM
THETA2=EBETA
THETA1=THETA2*57.2958
THETA2=THETA1*57.2958
DELV=(EMAX+EMIN)/2.
SIGMAX=2.*EMU(I)*EMAX+ELAM(I)*2.*DELV
SIGMIN=2.*EMU(I)*EMIN+ELAM(I)*2.*DELV
SHEAR=(SIGMAX+SIGMIN)/2.
HOOPE=0.
HOOPS=0.
IF(IGEOM.EQ.1) GO TO 205
QE=QE-NODE
PE=PE-NODE
QE=QE-NODE
HOOPE=(UO+UP+UQ)/(X(OE)+X(PE)+X(QE))
DELV=(HOOPE+EMAX+EMIN)/3.
SIGMAX=2.*EMU(I)*EMAX+ELAM(I)*3.*DELV
SIGMIN=2.*EMU(I)*EMIN+ELAM(I)*3.*DELV
PRESS=(SIGMAX+SIGMIN+HOOPS)/3.
HOOPS=2.*EMU(I)*HOOPE+ELAM(I)*3.*DELV
IF(HOOPS.LT.SIGMAX*AND(HOOPS.GT.SIGMIN) SHEAR=(SIGMAX-SIGMIN)/2.
IF(HOOPS.GT.SIGMAX) SHEAR=(HOOPS-SIGMIN)/2.
IF(HOOPS.LT.SIGMIN) SHEAR=(SIGMAX-HOOPS)/2.
WRITE(6,214)I,SIGMAX,SIGMIN,EMAX,EMIN,THETA1,THETA2,HOOPS,HOOPE,
1SHEAR,PRESS

```

```

FET07440
FET07450
FET07460
FET07470
FET07480
FET07490
FET07500
FET07510
FET07520
FET07530
FET07540
FET07550
FET07560
FET07570
FET07580
FET07590
FET07600
FET07610
FET07620
FET07630
FET07640
FET07650
FET07660
FET07670
FET07680
FET07690
FET07700
FET07710
FET07720
FET07730
FET07740
FET07750
FET07760
FET07770
FET07780
FET07790
FET07800
FET07810
FET07820
FET07830
FET07840
FET07850
FET07860
FET07890
FET07900
FET07910
FET07920
FET07930

```



```

214 13X, E11.4, 2X, I3, 3X, E11.4, 2X, E11.4, 2X, E11.4, 1X, F7.2, 2X, F7.2,
      13X, E11.4, 2X, E11.4, 3X, E11.4, 4X, E11.4)
      SIGX=2.*EMU(I)*EX+ELAM(I)*{(EX+EY)}
      SIGY=2.*EMU(I)*EY+ELAM(I)*{(EX+EY)}
      SIGXY=2.*EMU(I)*EXY
      WRITE(6, 950) SIGX, SIGY, SIGXY
950  FORMAT(12X, E11.4, 2X, E11.4, 2X, E11.4)
200  CONTINUE
2001 RETURN
      END
FET 07940
FET 07950
FET 07960
FET 07970
FET 07980
FET 07990
FET 08000
FET 08010
FET 08020
FET 08030
FET 08040

```


FET08060
 FET08070
 FET08080
 FET08090
 FET08100
 FET08110
 FET08120
 FET08130
 FET08140
 FET08150
 FET08160
 FET08170
 FET08180
 FET08190
 FET08200
 FET08220
 FET08230
 FET08240
 FET08250
 FET08260
 FET08270
 FET08280
 FET08290
 FET08300
 FET08310
 FET08320
 FET08330
 FET08340
 FET08350
 FET08360
 FET08370
 FET08380
 FET08390
 FET08400
 FET08410
 FET08420
 FET08430
 FET08440
 FET08450
 FET08460
 FET08470
 FET08480
 FET08490
 FET08500
 FET08510
 FET08520
 FET08530
 FET08540
 FET08550

```

SUBROUTINE QPLOT (LINES,L,X,FILL,IHR,NPT,RNG,DMIN,DAY1)
C
C PRINTER PLOT OF DISPLACEMENTS OF SURFACE NODES
C
DIMENSION X(L),LINE(127),ICHAN(10),CMNT(20)
DIMENSION IAXIS(100)
DATA IBLANK,'IIII',,,'IIII',/
DATA ICHAN/,,,'NNNN',,,'0000',,,'4444',,,'5555',,,'6666',,,'7777',,
1,7777',,,'8888',,,'9999',/
DATA IDOT, IDASH/,,,'',,/,
DO 32 I=1,10
DO 34 J=1,9
34 IAXIS(10*(I-1)+J)=IDOT
32 IAXIS(10*I)=IDASH
IF(NPT.EQ.8)GO TO 22
WRITE(6,100)
FORMAT(1H1)
22 WRITE(6,12)
FORMAT(1H0)
11 WRITE(6,11) (IAXIS(JJ),JJ=1,100)
FORMAT(28X,100A1)
DO 6 I=1,L,1
IF(X(I).GE.0)GO TO 6
IHR=IHR+1
IF(IHR.EQ.1)GO TO 7
DMIN=X(I)
IF(DMIN.GE.RNG)GO TO 6
RNG=DMIN
GO TO 6
RNG=X(I)
CONTINUE
DO 13 I=1,L,1
X(I)=X(I)-RNG
CONTINUE
B=0.0
DO 5 I=1,L,1
IF(X(I).GT.B) B=X(I)
DO 30 K=1,L,1
DO 10 I=1,100,1
LINE(I)=IBLANK
INTEG=1.0+X(K)*FILL/8
IF(INTEG.GT.100)INTEG=100
LINE(JAY1)=IIII
LINE(INTEG)=ICHAN(I)
X(K)=X(K)+RNG
WRITE(6,43) K,X(K),(LINE(I),I=1,100)
43 FORMAT(1X,13,2X,E11.4,11X,100A1)
CONTINUE
WRITE(6,12)
FORMAT(6,11) (IAXIS(JJ),JJ=1,100)

```


FET08560
FET08570
FET08580
FET08590

WRITE(6,205)
FORMAT(1H1)
RETURN
END

205

BIBLIOGRAPHY

1. Carey, G.F. and Martin, H.C., Introduction to Finite Element Analysis, McGraw-Hill, 1973.
2. Crowley, F.A., Ossing, H.A. and Cabiness, G.H., Precursory Siloed Missile Geokinetic Study Hill, Air Force Base, Utah, Air Force Surveys in Geophysics, Vol. 245, Sep 1972.
3. Dieterich, J.H., Documentation ASAPS Subroutine, National Center for Earthquake Research Program Library, Sep 1970.
4. Fix, G.J. and Strang, G., An Analysis of the Finite Element Method, Prentice-Hall, 1973.
5. Froberg, C.E., Introduction to Numerical Analysis, Addison-Wesley, 1965.
6. Grant, F.S. and West, G.F., Interpretation Theory In Applied Geophysics, McGraw Hill, 1965.
7. Mayer-Rosa, D., Travel-Time Anomalies and Distribution of Earthquakes Along the Calveras Fault Zone, California, Bulletin of the Seismological Society of America, Vol. 63, pp. 713-729, April 1973.
8. Melchior, P., The Earth Tides, Pergamon Press, 1966.
9. Smith, G.N., An Introduction to Matrix and Finite Element Methods in Civil Engineering, Applied Science Publishers, 1971.
10. Smith, P.J., Topics In Geophysics, The MIT Press, 1973.
11. Stewart, S.W., Preliminary Comparison of Seismic Travel Times and Inferred Crustal Structures Adjacent to the Diablo and Gablin Ranges of Central California, Stanford University Publications in the Geological Sciences, Vol. 11, pp. 218-230, 1968.
12. Wood, M.D., The Influence of Ocean Tidal Loading on Solid Earth Tides and Tilts in the San Francisco Bay Region, California, Ph.D. Thesis, Stanford University, 1969.
13. Wood, M.D., Allen, R.V. and Allen, S.S., Methods for Prediction and Evaluation of Tidal Tilt Data from Borehole and Observatory Sites Near Active Faults, Phil. Trans. R. Soc., London, Vol. 274, pp. 245-252, 1973.

14. Tide Harmonic Constants, International Hydrographic Bureau, Monaco, July 1953.
15. Zienkiewicz, O.C. and Cheung, Y.K., The Finite Element Method In Structural and Continuum Mechanics, McGraw-Hill, 1967.

INITIAL DISTRIBUTION LIST

	No. Copies
1. Defense Documentation Center Cameron Station Alexandria, Virginia 22314	2
2. Library, Code 0212 Naval Postgraduate School Monterey, California 93940	2
3. Department Chairman, Code 55 Department of Operations Research and Administrative Sciences Naval Postgraduate School Monterey, California 93940	2
4. Associate Professor Donald R. Barr, Code 55 Bn Department of Operations Research and Administrative Sciences	1
5. Associate Professor Rex H. Shudde, Code 55 Su Department of Operations Research and Administrative Sciences Naval Postgraduate School Monterey, California 93940	1
6. Captain Robert C. Foos 13060 Luber Street Salinas, California 93901	1
7. U.S. Army Military Personnel Center Attn: DAPC-OPD-PD-CS 200 Stovall Street Alexandria, Va. 22232	1
8. Chief of Naval Personnel Attn: Pers 11b Department of the Navy Washington, DC 20370	1
9. Dr. M. Darroll Wood National Center for Earthquake Research 800 Menlo Ave. Menlo Park, Ca. 94025	1



Thesis
F5767 Foos
c.1

160101

Modeling an input-
output geokinetic
system utilizing a
finite element approach.

Thesis
F5767 Foos
c.1

160101

Modeling an input-
output geokinetic
system utilizing a
finite element approach.

thesF5767

Modeling an input-output geokinetic syst



3 2768 000 99905 6

DUDLEY KNOX LIBRARY